Improving the Initial Conditions of Hydrological Model with Reanalysis Soil Moisture Data

Lingxue Liu [1, †], Tianqi Ao [1,2, †], Li Zhou [2, *]

[1] Institute for Disaster Management and Reconstruction, Sichuan University-Hong Kong Polytechnic University, Chengdu 610065, China
[2] State Key Laboratory of Hydraulics and Mountain River Engineering, College of Water Resource & Hydropower, Sichuan University, No.24 South Section 1, Yihuan Road, Chengdu 610065, China

† These authors contributed equally to this work.

Correspondence to: Li Zhou (zhouli.scu@gmail.com)

Abstract. The initial conditions (e.g., soil moisture content) of the hydrological model, which is usually obtained from the warm-up of the hydrological modeling, significantly impact the simulation efficiency. However, spending the valuable data in warm-up instead of calibration and validation is luxurious. In order to improve hydrological simulation efficiency in the case of no warm-up phase, this paper proposes a methodology to fill the gap via improving the initial conditions of the hydrological model using an alternative global soil moisture dataset. Specifically, three soil moisture (SM) variables of the initial conditions from the Block-wise use of the TOPMODEL (BTOP) model and EAR5-Land reanalysis data were adopted and conducted correlation analysis. Several traditional curve-fitting functions and the state-of-art technical, long-short term memory (LSTM), were applied to develop the relationship between BTOP and EAR5-Land SM variables in the Fuji and Shinano River Basin, Japan. Furthermore, four configured hydrological simulations evaluated the benefits of the proposed methodology for improving the initial conditions. As a result, LSTM outperforms the traditional curve-fitting method in constructing the relationship between variables in time and space. Moreover, the hydrological simulation cases using the initial conditions related to the SM from the ERA5-land performs better than the case without the warm-up phase, and the simulated discharge process approaches the "optimal" case with the warm-up phase. It is confirmed that the proposed methodology helps improve the initial conditions of the hydrological model using reanalysis soil moisture data.

Keywords. *BTOP model, ERA5-Land, model warm-up, Long-short term memory (LSTM), ungauged basin*

1 Introduction

Hydrological model is an essential tool to explore the physical law of hydrological process (Refsgaard, 1997; Senarath et al., 2000) and to provide valuable simulated results for various purposes such as drought and flood monitoring (Chen et al., 2018), water resources and irrigation management (Grové, 2019), and water environmental pollutant migration (Basheer, 2018). It needs to be calibrated to minimize the uncertainty before application (Gupta et al., 2009). One of the critical

impacts on hydrological modeling is the initial conditions (e.g., soil moisture content) which affect the simulation efficiency (e.g., stability and convergence) significantly, especially at the beginning of the hydrological simulation (Berthet et al., 2009; Bui et al., 2021). However, the issue of initial conditions has not been well solved due to various uncertainties from complex natural conditions, hydrological processes, and insufficient data (Beven and Binley, 1992; Cloke et al., 2003; Beven, 2006).

35 Generally, the initial conditions are often acquired from the warm-up of the hydrological model, which is a process adjusting the initial conditions of the model from the estimated state to the "optimal" state to reduce the impact of the initial state on the hydrological simulation (Kim et al., 2018). Usually, it is challenging to balance the period of model warm-up between data utilization and warm-up efficiency. Furthermore, the model warm-up period for daily simulation was usually set to one or two years at least (Boufala et al., 2019; Paul et al., 2020; Yu et al., 2019), or even several years (Erraioui et al., 2020;

40 Carlos Mendoza et al., 2021). This is highly extravagant to the vast ungauged basins worldwide, especially for the developing countries and mountainous areas. Therefore, it would significantly improve the hydrological simulation if the warm-up period could be shortened or skipped.

Soil moisture (SM) is a crucial variable among the initial conditions which affects the hydrological processes significantly as essential as precipitation (Kim et al., 2018; Niroula et al., 2018). Compared with other water cycle components, although the

45 total mass of soil water content is small, it affects the climate system by controlling the interaction of water, energy, and carbon flux between the land surface and the atmosphere (Seneviratne et al., 2010). Although the International Soil Moisture Network (ISMN) established a global in-situ soil measurement database for the use of improving satellite SM products and climate, land surface, and hydrological models (Dorigo et al., 2011, 2013), it has apparent limitations due to the poor spatial coverage and uneven distribution worldwide (Miralles et al., 2012; Nguyen et al., 2017). With the advancement of

50 technology, the satellite SM products and reanalysis data from the land surface model (LSM) have been significantly improved (Mousa and Shu, 2020; Wu et al., 2021; Dorigo et al., 2017; Muñoz Sabater et al., 2021), which allows the possibility to connect them with hydrological model SM variables.

Considerable work has been done about the initial conditions of the hydrological model on some subjects, such as the impact on ensemble streamflow prediction (Li et al., 2009; Roulin and Vannitsem, 2015; Piazzi et al., 2021; Donegan et al., 2021),

55 using data assimilation to improve the initial conditions for ensemble streamflow prediction (Dechant and Moradkhani, 2011; Cho and Kim, 2022; Muñoz et al., 2022), and employing alternative SM data (e.g., satellite, reanalysis) into the hydrological model directly (Muñoz et al., 2022; Massari et al., 2014; Setti et al., 2020). To our best knowledge, however, none of them addressed the issue of how to improve the initial conditions (e.g., soil moisture content) of the hydrological model with other datasets via developing their relationship. Therefore, this paper aims to propose a methodology to fill this gap, which could

60 improve the hydrological simulation by obtaining the initial conditions of the hydrological model from other datasets with proper process. In Sect. 2, we describe the material used in this study: two river basins in Japan, the Block-wise use of the TOPMODEL (BTOP) model, and the ERA5-Land dataset. The methodology is provided in Sect. 3, which employs six curve-fitting functions and the state-of-art deep learning technology, long short-term memory (LSTM) method to develop the

relationship between BTOP and EAR5-Land SM variables, and a configuration of hydrological simulation is designed for illustrating the importance of initial conditions, model warm-up, and the benefits of the proposed methodology. Sect. 4 describes the results and discussion of correlation analysis, relationship development, hydrological simulation, etc. Finally, we present the conclusions in Sect. 5.

2 Material

2.1 Study area

In this paper, we employed two major river basins in Japan as they have adequate hydro-meteorology data to achieve the goals of this study. As shown in Figure 1, the Fuji River Basin (FRB) and Shinano River Basin (SRB) are located in the central part of the Honshu island. They originate from the Japanese Alps, known as Japan's peak area.

The FRB flows through Nagano, Yamanashi, and Shizuoka prefectures, with a river length of 128 km and a drainage area of approximately 3570 km^2. It flows into the Pacific Ocean at Suruga bay, and the downstream section Kitamatsuno has a mean annual flow of 63.2 m^3/s. The average temperature of summer and winter are 26°C and 3°C, respectively (Shrestha and Kazama, 2006). Kofu Plain, which lies upstream of FRB, receives an average annual rainfall of 1100 mm. The middle and lower reaches of FRB have an average annual rainfall of 2000 and 2500 mm, respectively. The basin terrain is steep, with 90% of the area being mountainous or hilly. There are many peaks in the basin, including Japan's highest and world-famous mountain, Mt. Fuji, with an altitude of 3776 m.

The Shinano River is Japan's longest (367 km) and third-largest drainage area basin (11900 km^2). It originates at the foot of Kobushi Mountain in the Alps of Honshu Island, flows through Nagano and Niigata prefectures, and enters the Sea of Japan. The annual average flow of the Ojiya section is 503 m^3/s. The upper part of the SRB is called the Chikuma River Basin (CRB), which has a river length of 214 km and a drainage area of 7163 km^2, accounting for 58% and 60% of the SRB, respectively. In the upstream of CRB, it is surrounded by mountains, and there is only 10% of the land is flat for agriculture. The inland climate is remarkable, and the precipitation is low. The annual average precipitation in Nagano City is only 938 mm. However, the downstream part of SRB on the Niigata side has a unique climate in coastal areas of Japan. The annual average precipitation in Nagaoka City is 2310 mm. The abundant water and fertile soil make this area one of the best rice-producing areas in Japan.

2.2 Hydrological model: BTOP model

2.2.1 Brief introduction

The Block-wise use of the TOPMODEL (BTOP model) is based on the well-known semi-distributed hydrological model-TOPMODEL (Beven and Kirkby, 1979). It has been continually developed (Ao et al., 2006; Zhou et al., 2006; Takeuchi et al., 2008; Zhang et al., 2018) and applied to various basins worldwide (Magome et al., 2015; Gusyev et al., 2016; Liu et al.,

2020) for varies of purposes such as water resource management (Hapuarachchi et al., 2008), flood and drought monitoring (Zhou et al., 2021) since 1999 when it was first proposed in the University of Yamanashi, Japan (Takeuchi et al., 1999; Ao et al., 1999). The BTOP model is a semi-physically, reliable, and straightforward hydrological model, and its parameters have physically interpretation which could represent the influence of underlying surfaces such as vegetation, land use, soil properties, and soil moisture (Takeuchi et al., 2008; Wang et al., 2010; Zhu et al., 2021). These features allow the possibility of connecting the model simulated SM variables with other datasets such as reanalysis and satellite SM data.

2.2.2 Initial conditions and soil moisture-related variables

As shown in Figure 2a, the BTOP model defines the area above the ground surface covered by the plant canopy as a vegetation area and divides the subsurface aeration zone into three parts: the root zone, the unsaturated zone, and the saturated groundwater zone (Takeuchi et al., 2008). Table 1 describes the initial condition variables of the BTOP model, which could represent the basic information of underlying surface such as discharge, soil moisture, snow cover at each grid. This study focuses on the soil moisture related variables in the BTOP model: root zone storage (S_{rz}, m), unsaturated zone storage (S_{uz}, m), and saturation deficit (SD, m).

① Storage in root zone: S_{rz}

The root zone storage at grid i and time step t is calculated by the equation below:

$$S_{rz}(i,t)=S_{rz}(i,t-1)+\Delta t\left(P_a(i,t)-q_{ofh}(i,t)-ET(i,t)-q_{rz}(i,t)\right) \tag{1}$$

where $S_{rz}(i,t-1)$ is the root zone storage at time step $t-1$; $P_a(i,t)$ is the net rainfall; $q_{ofh}(i,t)$ is the hortonian overland flow; $ET(i,t)$ is the actual evapotranspiration from root zone; $q_{rz}(i,t)$ is the storage excess of the root zone at time step t.

② Storage in unsaturated zone: S_{uz}

The unsaturated zone storage at grid i and time step t can be represented by the following equation:

$$S_{uz}(i,t) = S_{uz}(i,t-1)+\left[q_{rz}(i,t)-q_{of}(i,t)-q_v(i,t)\right]\Delta t \tag{2}$$

where $S_{uz}(i,t-1)$ is the unsaturated zone storage at time step $t-1$; $q_{of}(i,t)$ is the saturation excess runoff flux; $q_v(i,t)$ is groundwater recharge at time step t.

③ Saturation deficit: SD

The saturation deficit at grid i and time step t is updated by the following equation:

$$SD(i,t) = SD(i,t-1)-\left(q_{rz}(i,t)+q_v(i,t)-q_b(i,t)\right)\Delta t \tag{3}$$

where $SD(i,t-1)$ is the saturation deficit at time step $t-1$; $q_b(i,t)$ is the base flow at time step t.

2.3 Model input data

2.3.1 Precipitation and discharge data

120   This study collected daily precipitation and discharge data from 2002 to 2011 from the Japan Meteorological Agency (JMA) and the Ministry of Land, Infrastructure, Transport and Tourism (MLIT). As shown in Figure 1, 26 and 77 precipitation stations were selected in FRB and SRB, respectively. Moreover, we employed two and seven discharge stations in FRB and SRB according to the basin area and data quality, making two and seven subbasins for each. For the model simulation, we set 2002 as the model warm-up period. In addition, 2003-2007 and 2008-2011 are set as calibration and validation periods.

125   #### 2.3.2 Other input data

We adopted 500 m and 1000 m resolution in FRB and SRB, respectively, for the model simulation, considering the data representation and computing time. Therefore, all the following data were resampled to the two resolutions above. The Digital Elevation Model (DEM) was obtained from Multi-Error-Removed Improved-Terrain (MERIT) DEM with an original resolution of three seconds (90 m at the equator) (Yamazaki et al., 2017). The BTOP model employed the MODIS-IGBP
130   Land Cover map (original resolution: 500 m) as land cover data (Friedl and Sulla-Menashe, 2019). Normalized Difference Vegetation Index (NDVI) and Leaf Area Index (LAI) came from the National Oceanic and Atmospheric Administration (NOAA) of the United States (Vermote et al., 2014) with a resolution of 0.05 degrees. Soil properties were obtained using the soil map (at a scale of 1:5 million) of the Food and Agriculture Organization (FAO). The Climate Research Unit (CRU) provided meteorological data (Harris et al., 2020) with a resolution of 0.25 degrees, such as temperature, radiation, humidity,
135   wind speed, and vapor pressure, for the evaporation module of BTOP model (Zhou et al., 2006) to generate potential interception evaporation (PET_0) and potential evapotranspiration (PET).

2.4 Reanalysis soil moisture data: ERA5-Land

The European Centre for Medium-Range Weather Forecasts (ECMWF) produces an enhanced global dataset for the land component of the 5th generation of European ReAnalysis (ERA5), called ERA5-Land (Muñoz Sabater et al., 2021). It covers
140   the same period (January 1950 to near real-time) and temporal resolution (hourly) as ERA5 (Hersbach et al., 2020). Compared with ERA5, ERA5-Land runs at enhanced resolution (0.1°, 9 km vs. 31 km in ERA5) without coupling to the ECMWF's Integrated Forecasting System, making it computationally affordable and lighter to handle. Moreover, it better describes the hydrological cycle, particularly with enhanced soil moisture, allowing it to broadly utilize various purposes such as SM monitoring and enhancing hydrological simulation. Unfortunately, to the authors' best knowledge, the research
145   related to the SM from the ERA5-Land has not been reported in Japan. However, in some areas which have similar climatic characteristics with the study area in this paper, the ERA5-Land SM data showed a better performance than many other datasets such as Global Land Data Assimilation System (GLDAS-2.1) (Wu et al., 2021), Advanced Scatterometer (ASCAT)

(Beck et al., 2020), and Soil Moisture and Ocean Salinity (SMOS) (Pablos et al., 2021). Therefore, the ERA5-Land dataset is worthy of being used to fulfill the objectives of this study.

150 Figure 2b shows the SM layer structure of ERA5-Land. It is divided into four layers: 0-7cm, 7-28cm, 28-100cm, and 100-289 cm. Moreover, each layer contains the soil moisture content (water storage) of *S1* to *S4*. We downloaded the hourly SM data from 2002 to 2011 from the Climate Data Store, Copernicus program (Muñoz Sabater, 2019). Then we shifted the ERA5-Land SM data to the Japan Standard Time (JST, UTC+9) and converted hourly to daily data to consistent the temporal with BTOP simulated variables. Moreover, to compare ERA5-Land SM with BTOP SM variables, we converted

155 the original unit (m^3/m^3) to meter by multiplying the depth of each corresponding layer under the assumption that the water content is evenly distributed in each layer (Brouwer et al., 1985).

3 Methodology

We propose a methodology shown in Figure 3 to achieve the objectives of this study. Firstly, four hydrological simulation cases are configured to build a comprehensive experiment and evaluation system for proving the importance of model warm-

160 up for hydrological simulation (Case 1 and 2), and whether it is possible to utilize alternative SM data (ERA5-Land) to improve the initial conditions of the hydrological model or not (inter-comparison of four cases). As shown on the right side of the framework, the SM variables of BTOP model and EAR5-Land are comprehensively analyzed in temporal and spatial. Then six traditional curve-fitting functions and cutting-edge technology, long-short term memory (LSTM), are used for developing the relationship of SM variables between BTOP model and EAR5-Land at both basin- and grid-scale. Finally, a

165 comprehensive evaluation is conducted for verifying the relationship development of SM variables between BTOP model and ERA5-Land, and an inter-comparison and evaluation is carried out for hydrological simulations with different initial conditions and warm-up processes.

3.1 Case configuration of hydrological simulations

We configure four hydrological simulation cases for FRB and SRB. The details are shown in Table 2. They share the exact

170 calibration (2003-2007) and validation period (2008-2011), and all cases are auto-calibrated by shuffled complex evolution (SCE-UA) method (Duan et al., 1994) with approximately ten thousand irritations for eight simulations each (four cases for two basins). Case 1 employs 2002 as the warm-up period. We consider its simulated variables are the most representative of the hydrological model. Therefore, it is regarded as the "optimal" case and provides the referee SM variables for the correlation analysis and relationship development with ERA5-Land SM data. Case 2 is the control test conducting the

175 simulation without warm-up to verify the warm-up effect for the hydrological model. Case 3 and 4 take the SM variables processed from processed ERA5-Land by using traditional curve-fitting and LSTM methods as the initial condition of BTOP model, respectively.

3.2 Correlation analysis

Before the relationship development of BTOP and EAR5-Land SM variables, a comprehensive correlation analysis should be carried out at different spatial (grid, sub-basin, basin) and temporal (daily and annual average daily) scales, which employs Pearson correlation coefficient (R) as the performance index. The daily SM data is from 2003-2011, covering the calibration and validation period. It should be noted that the outputs of BTOP model (500 and 1000 m for FRB and SRB, respectively) are resampled to 0.1° to be consistent with EAR5-Land, and all variables are processed using Min-max normalization technical (Jain et al., 2005; Antanasijevic et al., 2014). Three correlation analysis experiments (EXP) are conducted as the following description.

(1) EXP 1: analyzing one by one.

Three BTOP SM variables (S_{rz}, S_{uz}, SD) are analyzed with four EAR5-Land variables ($S1$, $S2$, $S3$, $S4$) successively.

(2) EXP 2: relating BTOP SM variables to the combination of EAR5-Land SM variables.

Many papers regarded the part between the ground surface to 100 cm below as the root zone (Bai et al., 2021; Pradhan, 2019; Qi et al., 2019). Moreover, in the BTOP model, S_{rz} represents the storage in the root zone. Therefore, from the physical concept and the water content structure shown in Figure 2, it is worth connecting S_{rz} with the sum of $S1$, $S2$, and $S3$, denoted as Sa in this paper. On the other hand, SD represents the saturation deficit in the BTOP model. Thus, we assume that its concept is similar to the value of ERA5-Land soil depth (289 cm) minus Sa, which is expressed as Sb.

(3) EXP 3: relating S_{uz} to S_{rz} and SD.

As for the S_{uz}, there is no apparent physical meaning to support its connection to ERA5-Land SM variables. Nevertheless, suppose we could get the relationship between one of the BTOP variables and ERA5-Land SM variables. In that case, it is not challenging to develop a relationship among the BTOP SM variables as they usually have a strong connection. Therefore, experiment three is designed to connect the S_{uz} with S_{rz} or SD. This could also be an alternative solution for other hydrological models when conducting this methodology.

3.3 Relationship development methods

This study employs two methods (curve-fitting and LSTM) to develop the relationship of SM variables between BTOP and EAR5-Land at two spatial scales: grid- (0.1°) and basin-scale. Specifically, the grid-scale applies the relationships developed by each grid to the corresponding grid, while the basin-scale uses the relationship developed by basin-average data for each grid. We take the model calibration period (2003-2007) and validation period (2008-2011) as the training and test period for developing the relationship, respectively.

3.3.1 Curve-fitting functions

Curve-fitting is a process of fitting the measured points by the appropriate functions to minimize the distance between the observed and fitted points (Ueng et al., 2007; Adnan et al., 2020). The commonly used curve types such as polynomial,

logarithmic, and power functions are always hard to express complex data distributions well (Pourkarimi et al., 2011). The spline fitting was proposed based on the practical piecewise polynomials (Dierckx, 1981). The widely applied and improved cubic spline fits each piece segmented by the knots with cubic polynomial, which is similar to the piecewise polynomials. However, there are some restrictions that the polynomials, their first-order and second-order derivatives are all continuous at the knots to generate a smooth curve (Lavery, 2002, 2000; Zhanlav and Mijiddorj, 2018). Moreover, due to the unstable polynomial functions and the fewer measured points, over-fitting often occurs in the boundary region. Sequentially, an additional restriction that the function outside the boundary knots is linear was added, and the corresponding spline is called a natural spline. It allows the polynomials to extend smoothly beyond the boundary knots (Huang et al., 2018).

Combined with the scatter distribution of the well-correlated variable combinations obtained by the correlation analysis (as shown in Sect. 4.2), we selected six commonly used functions in Table 3. They are applied for the relationship development at grid- and basin-scale in Sect. 4.3.

3.3.2 Long short-term memory (LSTM)

LSTM is developed to address the problem of vanishing gradient in recurrent neural networks (RNN), and has been widely used in various kinds of tasks, including speech recognition and sentence embedding (Arslan and Barışçı, 2019; Palangi et al., 2016; Graves et al., 2013), correlation analysis (Deng et al., 2020; Yang et al., 2020), and hydrometeorological forecast (Yin et al., 2021; Ni et al., 2020). LSTM has a special internal structure design which includes two states (cell state, hidden state) for information storage and three gates (input gate, forget gate, and output gate) for information addition or deletion, making it a strong learning ability and applicable for sequence data learning (Yu et al., 2019; Sherstinsky, 2020). Referring to Keras (Chollet and Others, 2015), a deep learning algorithm written in python, LSTM conducted in this study is described in Figure 4. The input variables include precipitation (P), potential evapotranspiration (PET), potential intercept evaporation (PET_0), leaf area index (LAI), and the water storage of four layers ($S1$, $S2$, $S3$, $S4$) from the ERA5-Land, while the outputs are S_{rz}, S_{uz} and SD of BTOP model.

3.4 Evaluation scheme

3.4.1 Evaluation of the fitting method and developed relationship

(1) General evaluation criteria

The Pearson correlation coefficient (R) is commonly used for correlation analysis as it can well represent their relationship strength between two variables (Al-Yaari et al., 2017; Gruber et al., 2020). Moreover, several indicators are selected as evaluation criteria, such as relative mean absolute error ($rMAE$), relative root mean square error ($rRMSE$), normalized standard deviation (NSD), normalized root mean square deviation ($NRMSD$), and coefficient of determination (R^2). The following equations show the details of the evaluation indicators:

$$R = \frac{\sum_{i=1}^{n}\left(X_i^B - \overline{X^B}\right)\left(X_i^E - \overline{X^E}\right)}{\sqrt{\sum_{i=1}^{n}\left(X_i^B - \overline{X^B}\right)^2}\sqrt{\sum_{i=1}^{n}\left(X_i^E - \overline{X^E}\right)^2}} \tag{4}$$

$$rMAE = \frac{MAE}{\overline{X^B}} = \frac{\sum_{i=1}^{n}\left|X_i^E - X_i^B\right|}{\sum_{i=1}^{n} X_i^B} \tag{5}$$

$$rRMSE = \frac{RMSE}{\overline{X^B}} = \sqrt{\frac{n\sum_{i=1}^{n}\left(X_i^E - X_i^B\right)^2}{\left(\sum_{i=1}^{n} X_i^B\right)^2}} \tag{6}$$

$$NSD = \sqrt{\frac{\sum_{i=1}^{n}\left(X_i^E - \overline{X^E}\right)^2}{\sum_{i=1}^{n}\left(X_i^B - \overline{X^B}\right)^2}} \tag{7}$$

$$NRMSD = \frac{\sum_{i=1}^{n}\left|X_i^s - X_i^o\right|^2}{\sum_{i=1}^{n} X_i^{o2}} \tag{8}$$

where X^B are the BTOP SM variables; X^E are the ERA5-Land SM variables; i is the time step.

240   (2) Selection scheme of curve-fitting functions

To uniform the performance of each curve-fitting function, we develop an evaluation scheme as described as follows: Firstly, normalizing the five indicators shown above using Min-max normalization technical (Jain et al., 2005; Antanasijevic et al., 2014) to get the score values between 0 and 1. Secondly, it gives the exact weight of 0.2 to five each index to keep the optimal score as one still. Thirdly, assigning weights of 0.7 and 0.3 to test and training period, respectively, since we value

245   the test period more. To this point, the calculated scores of each function have been completed with an optimal value of 1. It should be noted that the fitting process is only conducted at the basin scale in the selection phase.

3.4.2 Evaluation of the hydrological simulation

As for the evaluation of hydrological simulation, not only the Nash-Sutcliffe Efficiency (*NSE*) (Nash and Sutcliffe, 1970) but also the improved Kling–Gupta efficiency (*KGE'*) (Gupta et al., 2009) are employed as the criteria to evaluate the

250   hydrological simulation efficiency among different configured cases. The equations are shown below:

$$NSE = 1 - \frac{\sum_{i=1}^{n}\left(Q_i^S - Q_i^O\right)^2}{\sum_{i=1}^{n}\left(Q_i^O - \overline{Q_i^O}\right)^2} \tag{9}$$

9

$$KGE' = 1 - \sqrt{(r-1)^2 + (\beta - 1)^2 + (\gamma - 1)^2}$$

(10)

where Q^s and Q^o represent the simulated and observed discharge respectively; r is the correlation coefficient, β is the bias ratio, γ is the variability ratio.

4 Results and discussion

4.1 SM variables of BTOP and ERA5-Land

255   As we described the methodology in Figure 3, BTOP SM variables (S_{rz}, S_{uz}, SD) acquired from hydrological simulation Case 1 are regarded as the referee data of model SM variables. This section analyzed them and four ERA5-Land SM variables ($S1$, $S2$, $S3$, and $S4$) from 2003 to 2011 at both temporal and spatial scales. According to the hydrological simulation performance of each section (see details Table S1), however, we only adopted the results of two stations in FRB (subbasin: FRB-1, FRB-2) and four stations in SRB (subbasin: SRB-1, SRB-2, SRB-3 SRB-4) for the following analysis process and hydrological
260   simulations due to the poor simulated performance in SRB-5, SRB-6, and SRB-7.

As shown in Figure 5 and Figure 6, the SM variables of BTOP and ERA5-Land have a certain relationship, regardless of the temporal or spatial scale. Specifically, despite the absolute values, in the view of temporal scale (Figure 5), daily changes of BTOP are more dramatic than ERA5-Land, and the ERA5-Land have a better interannual variability than BTOP in terms of annual average daily scale. From the aspect of spatial distribution (Figure 6), the BTOP variables have a more evident and
265   specific distribution than EAR5-Land due to a higher resolution. According to the definition of SD in BTOP (Takeuchi et al., 2008), the values of SD are negative in some areas (central FRB and SRB) due to land use of city area.

It should be noted that, since the BTOP and ERA5-Land variables are come from hydrological and land surface models, and the models' fundament are based on many conception assumptions instead of actual physical law (Liang et al., 1994; Albergel et al., 2012; Frassl et al., 2018; Muñoz Sabater et al., 2021), there is no "truth" value in this study. Moreover, the
270   absolute values of these seven variables are different; therefore, it is necessary to conduct several experiments of correlation analysis in the following section. In addition, as the spatial characteristics of BTOP and ERA5-Land are different, it is also necessary to develop their relationship at grid-scale instead of basin-scale only.

4.2 Correlation analysis of SM variables

4.2.1 EXP 1: Correlation of S_{rz}, S_{uz}, SD and $S1$, $S2$, $S3$, $S4$

275   Experiment one analyzed the correlation between BTOP and EAR5-Land SM variables successively to understand the relationships among them better. Figure 7 shows the scatterplots of the correlation results of EXP 1 at basin scale, while Fig. S1 and S2 are at sub-basin scale, which is similar to the basin scale. The S_{rz} has a significant positive correlation with $S1$, $S2$, and $S3$ in different (sub-) basins at a daily scale (the red dots and lines in Figure 7**a** and **b**, the values of R are around 0.5). In contrast, SD negatively correlates with EAR5-Land variables (the blue dots and lines in Figure 7**a** and **b**), especially the

280   correlation coefficient with $S4$ where the absolute value reaches 0.7 in FRB at daily scale. As for the S_{uz}, there is no apparent correlation with ERA5-Land at daily scale. Given the annual average daily scale (Figure 7**c** and **d**), the correlation between S_{uz} and ERA5-Land is stronger than the daily scale. However, it is not enough to support the relationship development between these two variables. Therefore, we conducted EXP 3 for S_{uz} which has poor connections with ERA5-Land SM variables, and the results are shown in Sect. 4.2.3.

4.2.2 EXP 2: Correlation of S_{rz} and Sa, SD and Sb

285   Although S_{rz} and SD have good correlations with each layer of ERA5-Land SM variables, the relationship development should use more reasonable correlated variable combinations with reliable physical meaning or interpretation as much as possible. Thus, EXP 2 illustrated the correlations of Srz and Sa, SD and Sb, which were constructed based on the physical interpretations. Figure 8 and Figure S3 show the basin- and subbasin-scale results, respectively. Same as EXP 1, the performance of the subbasin scale is similar to the basin scale. Although the performance of the annual average daily scale (Figure 8b) is not satisfied, the results of daily scale (Figure 8a) show a considerable close correlation as the values of R are more stable, and the dots are more gathered than EXP 1 (Figure 7a and b). It indicates that EXP 2 is more appropriate for the relationship development of S_{rz} and SD than EXP 1.

4.2.3 EXP 3: Correlation of S_{uz} and S_{rz}, SD

295   As the results of EXP 1 that no apparent connections are shown between S_{uz} and the EAR5-Land SM variable, EXP 3 was conducted to explore the relationship among BTOP variables since they have strong connections due to the model structure (Takeuchi et al., 2008; Hapuarachchi et al., 2008). The daily and annual average daily scatterplots of EXP 3 at basin scale are shown in Figure 9, while Fig. S4 shows the results of the subbasin scale, which are basically consistent with the basin scale. In the view of daily scale, as shown in Figure 9a, no apparent relationships are demonstrated between S_{uz} and S_{rz} or SD.

300   Nevertheless, from the aspect of the annual average daily scale, Figure 9b shows a strong connection between S_{uz} and SD, with the absolute correlation coefficients of 0.89 and 0.56 in FRB and SRB, respectively. Therefore, it is reasonable to take SD to develop the relationship with S_{uz} using the correlation information at the annual average daily scale.

It should be noted that the poor performance of simulated S_{uz} in this study might be caused by the model uncertainties or some other unknown reasons at the current stage. We must fix the possible problem in the BTOP model in future work.

305   However, EXP 3 still shows an alternative way to establish the relationship development for the variables that do not have adequate connections with other datasets like ERA5-Land.

4.2.4 Performance of correlation coefficients at grid-scale

Figure 10 shows the boxplots of the absolute correlation coefficients of all SM variables combinations from EXP 1-3 at grid-scale. In the view of S_{rz} as shown in Figure 10a, the daily scale performs better than the annual average daily scale, and the

310   results of S_{rz}-$S1$, S_{rz}-$S2$, S_{rz}-$S3$ are similar with S_{rz}-Sa at daily scale, which has a median R round 0.5. However, S_{rz}-Sa still

11

shows a slight advantage over others as it has physical interpretations explained in EXP 2, Sect. 3.23.2. Figure 10b shows the correlation results of SD. It's clear that SD-Sb outperforms others at daily scale. In the view of the annual average daily scale, it has a wide range of R and lower median value than daily scale as some grids do not have a good relationship with corresponding SM variables. As for S_{uz}, which does not have a considerable correlation with ERA5-Land SM variables, we conducted an additional experiment to connect the BTOP variables shown in Figure 10c together with all correlation results of S_{uz}. The correlation shows a significant improvement while using S_{uz}-SD at the annual average daily scale, in which the highest absolute R reaches 0.92 in the case of FRB-1.

Moreover, Figure 11 shows the spatial distribution of the absolute correlation coefficients at grid-scale in FRB and SRB. From the aspect of S_{rz} and SD, their relationships with Sa and Sb are prior choices for the following relationship construction under consideration of performance and physical mechanism. Looking at the results of S_{uz}-SD, there are some areas with pretty high correlations, while the city, plain areas with bad results. However, considering the poor connections between S_{uz} and ERA5-Land, S_{uz}-SD is still the best choice at the current stage. In summary, according to the correlation analysis results, the relationships of S_{rz} and Sa, SD and Sb, and S_{uz} and SD are chosen to develop the relationship formulas.

4.3 Relationship development of SM variables between BTOP and ERA5-Land

This section shows the results of the selection of six curve-fitting functions, the developed relationships using the selected curve-fitting functions and LSTM, and their performance at grid- and basin-scale.

4.3.1 Selection of curve-fitting functions

Table 4 shows the scores of each curve-fitting function in the two basins. In addition, Table S2-S4 present the developed formulas of three BTOP SM variables with different curve-fitting functions. For S_{rz}-Sa, the natural cubic spline outperforms other functions. In the view of SD-Sb, the quadratic polynomial has the best scores. They have a strong linear relationship, making the polynomial functions fit the relationship development best. From the S_{uz}-SD aspect, first-order polynomial and quadratic polynomial perform best in FRB and SRB, respectively. It is reasonable that the blue dots in Figure 9b show a more robust liner relationship in FRB than it is in SRB. Therefore, we employed the optimal curve-fitting functions for each basin and BTOP SM variables, as shown in the bold number in Table 4.

4.3.2 Performance evaluation of curve-fitting and LSTM

Figure 12 shows the performance evaluation results of selected curve-fitting and LSTM in FRB and SRB using the Talyor diagram (Taylor, 2001). Generally, the LSTM with grid-scale (blue dot) is the best among these relationship development methods, and the results developed by grid-scale outperform those by basin-scale in the test period as the dense circles are closer to REF than cross markers. Although, the LSTM at basin-scale (purple cross) shows a slighter poor performance than grid-scale (purple dot) in the test period. The test period achieves satisfying results with basin-scale (blue circle). Moreover, the LSTM with basin-scale also shows good spatial performance in Fig. S5, which presents a certain day of the spatial

distribution of BTOP SM variables and their predicted ones by curve-fitting and LSTM at both grid- and basin-scale. It demonstrates that the LSTM has the ability to represent spatial characteristics even conducting at basin scale. One reason is that the input factors include the variables that have spatial information, such as evapotranspiration and leaf area index. Thus, when this methodology is applied to a large basin or area, it is recommended to use LSTM with basin-scale to reduce the computation. From the aspect of S_{uz} shown in Figure 12c, it is evident that both methods show poorer performance than S_{rz} and SD. As we mentioned in Sect. 4.2.3, the performance of S_{uz} in the BTOP model needs to be improved in future work. Accordingly, the fitting results from the developed relationships based on LSTM and the curve-fitting method at grid-scale are applied to the configured hydrological simulations.

4.4 Inter-comparison and evaluation of configured hydrological simulations

Figure 13 shows the evaluation results of four configured hydrological simulations described in Table 2, and the specific values are presented in Table S5. Although it has a few differences in the view of R in calibration and validation period shown in the third column of Figure 13, Case 2 (blue lines) simulated without warm-up phase performs the worst from the aspect of NSE and KGE' compared to the referee Case 1 (red lines) shown in the first two columns in Figure 13. It indicates that the warm-up process is significantly necessary for the hydrological simulations. In the calibration and validation period shown in Figure 13a and b, Case 3 and 4 considerably improved the efficiency of runoff simulations compared to Case 2 except SRB-4, and the LSTM performs slightly better than the curve-fitting method.

To further address the impact of the initial conditions on the hydrological simulation, Figure 13c shows the results of the year 2003, which is the first year in the calibration period after the warm-up period. Case 3 and 4 utilizing ERA5-Land SM data to obtain the initial conditions significantly improve hydrological simulation efficiency. Specifically, given the mean value of seven simulated sub-basins shown in Table S5, Case 2 is the worst with a mean R of 0.45, while Case 1 is the best one with 0.71. Case 3 and 4 with R values of 0.67 is similar to Case 1. It indicates that the hydrological simulation could be considerably improved with improving initial conditions, especially in the warm-up period.

In general, the hydrological simulation results of BTOP model are considerably improved with improving initial conditions acquired from ERA5-Land SM variables compared to Case 2 which does not have a warm-up phase. This study conducted the optimal curve-fitting function and LSTM method to determine the relationship between BTOP and the ERA5-Land SM variable. Currently, lots of references have addressed the close correlation among satellite, reanalysis, model-simulated, or in-situ SM variables (Beck et al., 2020; Zhang et al., 2021; Ling et al., 2021). Therefore, the authors believe this methodology could be applied to other models or alternative datasets. Nonetheless, more work needs to be done in the future to address more models and datasets as a single model has obvious limitations (Orth et al., 2015).

13

5 Conclusions

In this paper, we proposed a methodology that well-utilizes the alternative global soil moisture data to improve hydrological simulation efficiency without warm-up by providing the initial conditions of the hydrological model with proper processes. The BTOP model and ERA5-Land reanalysis data were selected to represent the hydrological model and global soil moisture
375 dataset. Six discharge stations divided the subbasins and evaluated hydrological simulation in the Fuji River Basin and Shinano River Basin, Japan. Then, we comprehensively analyzed the correlation of BTOP and ERA5-Land SM variables and developed their relationships using traditional curve-fitting functions and the LSTM method. Finally, we demonstrate the benefits of the proposed methodology on the hydrological simulation. The conclusions are as follows:

(1) The warm-up is necessary for hydrological simulation if there is no other way to get the reasonable initial conditions at
380 the first time step in the calibration period.

(2) The initial conditions of the hydrological model could be obtained from the processed alternative SM data, which could improve the hydrological efficiency through shortening or skipping the warm-up phase.

(3) LSTM outperforms the traditional curve-fitting method, even using basin-scale to develop the relationship between BTOP model and EAR5-Land SM variables.

385 Moreover, we suppose the proposed methodology could be applied to any good quality data (e.g., reanalysis, satellite) in temporal and spatial to construct the related initial condition variables in the hydrological model or other models to improve the simulation efficiency. The benefits also cover the data-saving aspect, which is quite precious for the vast poorly- or un-gauged basins worldwide. However, it should be noted that, in this study, only one hydrological model and one global soil moisture dataset were employed to validate the proposed methodology. Future work should address more variables, models,
390 and datasets to validate its applicability further.

Author contributions

395 Lingxue Liu: Conceptualization, Methodology, Formal analysis, Data Curation, Visualization, Writing- original draft, Writing- review& editing. Tianqi Ao: Methodology, Formal analysis, Funding acquisition, Writing- review& editing, Supervision. Li Zhou: Conceptualization, Methodology, Formal analysis, Data Curation, Funding acquisition, Writing- original draft, Writing- review& editing.

References

Adnan, S.B.Z., Ariffin, A.A.M. and Misro, M.Y.: Curve fitting using quintic trigonometric Bézier curve, AIP Conference
410 Proceedings, 2266(1), 040009,2020.

Albergel, C., de Rosnay, P., Gruhier, C., Muñoz-Sabater, J., Hasenauer, S. and Isaksen, L. et al.: Evaluation of remotely sensed and modelled soil moisture products using global ground-based in situ observations, Remote Sens. Environ., 118, 215-226,2012.

Al-Yaari, A., Wigneron, J.P., Kerr, Y., Rodriguez-Fernandez, N., O'Neill, P.E. and Jackson, T.J. et al.: Evaluating soil
415 moisture retrievals from ESA's SMOS and NASA's SMAP brightness temperature datasets, Remote Sens. Environ., 193, 257-273,2017.

Antanasijevic, D., Pocajt, V., Peric-Grujic, A. and Ristic, M.: Modelling of dissolved oxygen in the Danube River using artificial neural networks and Monte Carlo Simulation uncertainty analysis, J. Hydrol., 519, 1895-1907,2014.

Ao, T., Ishidaira, H. and Takeuchi, K.: Study of Distributed Runoff Simulation Model Based on Block Type TOPMODEL
420 and Muskingum-Cunge Method, PROCEEDINGS OF HYDRAULIC ENGINEERING, 43, 7-12,1999.

Ao, T., Ishidaira, H., Takeuchi, K., Kiem, A.S., Yoshitari, J. and Fukami, K. et al.: Relating BTOPMC model parameters to physical features of MOPEX basins, J. Hydrol., 320(1-2), 84-102,2006.

Arslan, R.S. and Barışçı, N.: Development of Output Correction Methodology for Long Short Term Memory-Based Speech Recognition, Sustainability-Basel, 11(15), 4250,2019.

425 Bai, X., Jiang, Y., Miao, H., Xue, S., Chen, Z. and Zhou, J.: Intensive vegetable production results in high nitrate accumulation in deep soil profiles in China, Environ. Pollut., 287, 117598,2021.

Basheer, A.A.: New generation nano-adsorbents for the removal of emerging contaminants in water, J. Mol. Liq., 261, 583-

593,2018.

Beck, H.E., Pan, M., Miralles, D.G., Reichle, R.H., Dorigo, W.A. and Hahn, S. et al.: Evaluation of 18 satellite‑ and model‑
430   based soil moisture products using in situ measurements from 826 sensors, Hydrol. Earth Syst. Sc., 2020, 1-35,2020.

Berthet, L., Andréassian, V., Perrin, C. and Javelle, P.: How crucial is it to account for the antecedent moisture conditions in flood forecasting? Comparison of event-based and continuous approaches on 178 catchments, Hydrol. Earth Syst. Sc., 13(6), 819-831,2009.

Beven, K.: A manifesto for the equifinality thesis, J. Hydrol., 320(1-2), 18-36,2006.

435   Beven, K. and Binley, A.: The future of distributed models: Model calibration and uncertainty prediction, Hydrol. Process., 6(3), 279-298,1992.

Beven, K.J. and Kirkby, M.J.: A physically based, variable contributing area model of basin hydrology, Hydrological Sciences Bulletin, 1(24), 43-69,1979.

Boufala, M.H., El Hmaidi, A., Chadli, K., Essahlaoui, A., El Ouali, A. and Taia, S.: Hydrological modeling of water and soil
440   resources in the basin upstream of the Allal El Fassi dam (Upper Sebou watershed, Morocco), Modeling Earth Systems and Environment, 5(4), 1163-1177,2019.

Brouwer, C., Goffeau, A. and Heibloem, M., 1985. Irrigation Water Management : Training Manual No . 1 - Introduction to Irrigation. Food and Agriculture Organization of the United Nations, Rome.

Bui, M.T., Lu, J. and Nie, L.: Evaluation of the Climate Forecast System Reanalysis data for hydrological model in the
445   Arctic watershed Målselv, J. Water Clim. Change,2021.

Carlos Mendoza, J.A., Chavez Alcazar, T.A. and Zuñiga Medina, S.A.: Calibration and Uncertainty Analysis for Modelling Runoff in the Tambo River Basin, Peru, Using Sequential Uncertainty Fitting Ver-2 (SUFI-2) Algorithm, Air, Soil and Water Research, 14, 117862212098870,2021.

Chen, F., Crow, W.T., Bindlish, R., Colliander, A., Burgin, M.S. and Asanuma, J. et al.: Global-scale evaluation of SMAP,
450   SMOS and ASCAT soil moisture products using triple collocation, Remote Sens. Environ., 214, 1-13,2018.

Cho, K. and Kim, Y.: Improving streamflow prediction in the WRF-Hydro model with LSTM networks, J. Hydrol., 605, 127297,2022.

Chollet, F. and Others, 2015. Keras. GitHub. Available at: https://github.com/fchollet/keras.

Cloke, H.L., Renaud, J.P., Claxton, A.J., Mcdonnell, J.J., Anderson, M.G. and Blake, J.R. et al.: The effect of model
455   configuration on modelled hillslope – riparian interactions, J. Hydrol., 279(1-4), 167-181,2003.

Dechant, C.M. and Moradkhani, H.: Improving the characterization of initial condition for ensemble streamflow prediction using data assimilation, Hydrology and earth system sciences discussions, 8(4), 7207-7235,2011.

Deng, Y., Jiao, F., Zhang, J. and Li, Z.: A Short-Term Power Output Forecasting Model Based on Correlation Analysis and ELM-LSTM for Distributed PV System, Journal of Electrical and Computer Engineering, 2020, 1-10,2020.

460   Dierckx, P.: An Algorithm for Surface-Fitting with Spline Functions, IMA J. Numer. Anal., 1(3), 267-283,1981.

Donegan, S., Murphy, C., Harrigan, S., Broderick, C., Foran Quinn, D. and Golian, S. et al.: Conditioning ensemble

16

streamflow prediction with the North Atlantic Oscillation improves skill at longer lead times, Hydrol. Earth Syst. Sc., 25(7), 4159--4183,2021.

Dorigo, W., Wagner, W., Albergel, C., Albrecht, F., Balsamo, G. and Brocca, L. et al.: ESA CCI Soil Moisture for improved Earth system understanding: State-of-the art and future directions, Remote Sens. Environ., 203, 185-215,2017.

Dorigo, W.A., Wagner, W., Hohensinn, R., Hahn, S., Paulik, C. and Xaver, A. et al.: The International Soil Moisture Network: a data hosting facility for global in situ soil moisture measurements, Hydrol. Earth Syst. Sc., 15(5), 1675-1698,2011.

Dorigo, W.A., Xaver, A., Vreugdenhil, M., Gruber, A., Hegyiová, A. and Sanchis-Dufau, A.D. et al.: Global Automated Quality Control of In Situ Soil Moisture Data from the International Soil Moisture Network, Vadose Zone J., 12(3), vzj2012.0097,2013.

Duan, Q., Sorooshian, S. and Gupta, V.K.: Optimal use of the SCE-UA global optimization method for calibrating watershed models, J. Hydrol., 158(3), 265-284,1994.

Erraioui, L., Soufiane, T., Haida, S., Elmansouri, B. and Kamal, T., 2020. Semi-Distributed Modeling Of A Large Scale Hydrological System Using SWAT Model.

Frassl, M., Boehrer, B., Holtermann, P., Hu, W., Klingbeil, K. and Peng, Z. et al.: Opportunities and Limits of Using Meteorological Reanalysis Data for Simulating Seasonal to Sub-Daily Water Temperature Dynamics in a Large Shallow Lake, Water-Sui., 10(5), 594,2018.

Friedl, M. and Sulla-Menashe, D., MCD12Q1 MODIS/Terra+Aqua Land Cover Type Yearly L3 Global 500m SIN Grid V006 [Data set]. NASA EOSDIS Land Processes DAAC, https://doi.org/10.5067/MODIS/MCD12Q1.006(accessed on Jun. 10 2020)

Graves, A., Mohamed, A. and Hinton, G., 2013. Speech recognition with deep recurrent neural networks. 2013 IEEE International Conference on Acoustics, Speech and Signal Processing, pp. 6645-6649.

Grové, B.: Improved Water Allocation under Limited Water Supplies Using Integrated Soil-Moisture Balance Calculations and Nonlinear Programming, Water Resour. Manag., 33(1), 423-437,2019.

Gruber, A., De Lannoy, G., Albergel, C., Al-Yaari, A., Brocca, L. and Calvet, J.C. et al.: Validation practices for satellite soil moisture retrievals: What are (the) errors? Remote Sens. Environ., 244, 111806,2020.

Gupta, H.V., Kling, H., Yilmaz, K.K. and Martinez, G.F.: Decomposition of the mean squared error and NSE performance criteria: Implications for improving hydrological modelling, J. Hydrol., 377(1-2), 80-91,2009.

Gusyev, M., Gädeke, A., Cullmann, J., Magome, J., Sugiura, A. and Sawano, H. et al.: Connecting global- and local-scale flood risk assessment: a case study of the Rhine River basin flood hazard, J. Flood Risk Manag., 9(4), 343-354,2016.

Hapuarachchi, H.A.P., Takeuchi, K., Zhou, M., Kiem, A.S., Georgievski, M. and Magome, J. et al.: Investigation of the Mekong River basin hydrology for 1980 – 2000 using the YHyM, Hydrol. Process., 22(9), 1246-1256,2008.

Harris, I., Osborn, T.J., Jones, P. and Lister, D.: Version 4 of the CRU TS monthly high-resolution gridded multivariate climate dataset, Scientific Data, 7(1),2020.

17

Hersbach, H., Bell, B., Berrisford, P., Hirahara, S., Horányi, A. and Muñoz Sabater, J. et al.: The ERA5 global reanalysis, Q. J. Roy. Meteor. Soc., 146(730), 1999-2049,2020.

Huang, C., Wang, L., Yeung, R.S., Zhang, Z., Chung, H.S. and Bensoussan, A.: A Prediction Model-Guided Jaya Algorithm for the PV System Maximum Power Point Tracking, IEEE T. Sustain. Energ., 9(1), 45-55,2018.

Jain, A., Nandakumar, K. and Ross, A.: Score normalization in multimodal biometric systems, Pattern Recogn., 38(12), 2270-2285,2005.

Kim, K.B., Kwon, H. and Han, D.: Exploration of warm-up period in conceptual hydrological modelling, J. Hydrol., 556, 194-210,2018.

Lavery, J.E.: Univariate cubic Lp splines and shape-preserving, multiscale interpolation by univariate cubic L1 splines, Comput. Aided Geom. D., 17(4), 319-336,2000.

Lavery, J.E.: Shape-preserving, multiscale interpolation by univariate curvature-based cubic L1 splines in Cartesian and polar coordinates, Comput. Aided Geom. D., 19(4), 257-273,2002.

Li, H., Luo, L., Wood, E.F. and Schaake, J.: The role of initial conditions and forcing uncertainties in seasonal hydrologic forecasting, Journal of Geophysical Research, 114(D4),2009.

Liang, X., Lettenmaier, D.P., Wood, E.F. and Burges, S.J.: A simple hydrologically based model of land surface water and energy fluxes for general circulation models, Journal of Geophysical Research, 99(D7), 14415,1994.

Ling, X., Huang, Y., Guo, W., Wang, Y., Chen, C. and Qiu, B. et al.: Comprehensive evaluation of satellite-based and reanalysis soil moisture products using in situ observations over China, Hydrol. Earth Syst. Sc., 25(7), 4209-4229,2021.

Liu, L., Zhou, L., Li, X., Chen, T. and Ao, T.: Screening and Optimizing the Sensitive Parameters of BTOPMC Model Based on UQ-PyL Software: Case Study of a Flood Event in the Fuji River Basin, Japan, J. Hydrol. Eng., 25(9), 05020030,2020.

Magome, J., Gusyev, M.A., Hasegawa, A. and Takeuchi, K., 2015. River discharge simulation of a distributed hydrological model on global scale for the hazard quantification, Proc. 21st International Congress on Modelling and Simulation (MODSIM2015), Broadbeach, Queensland, Australia, pp. 1593-1599.

Massari, C., Brocca, L., Barbetta, S., Papathanasiou, C., Mimikou, M. and Moramarco, T.: Using globally available soil moisture indicators for flood modelling in Mediterranean catchments, Hydrol. Earth Syst. Sc., 18(2), 839--853,2014.

Miralles, D.G., van den Berg, M.J., Teuling, A.J. and de Jeu, R.A.M.: Soil moisture-temperature coupling: A multiscale observational analysis, Geophys. Res. Lett., 39(21), n/a-n/a,2012.

Mousa, B.G. and Shu, H.: Spatial Evaluation and Assimilation of SMAP, SMOS, and ASCAT Satellite Soil Moisture Products Over Africa Using Statistical Techniques, Earth and Space Science, 7(1),2020.

Muñoz Sabater, J., ERA5-Land hourly data from 1981 to present. Copernicus Climate Change Service (C3S) Climate Data Store (CDS), https://cds.climate.copernicus.eu/cdsapp#!/dataset/reanalysis-era5-land?tab=overview(accessed on Oct. 20 2021)

Muñoz Sabater, J., Dutra, E., Agustí-Panareda, A., Albergel, C., Arduini, G. and Balsamo, G. et al.: ERA5-Land: a state-of-

530   the-art global reanalysis dataset for land applications, Earth system science data, 13(9), 4349-4383,2021.

Muñoz, D.F., Abbaszadeh, P., Moftakhari, H. and Moradkhani, H.: Accounting for uncertainties in compound flood hazard assessment: The value of data assimilation, Coast. Eng., 171, 104057,2022.

Nash, J.E. and Sutcliffe, J.V.: River flow forecasting through conceptual models part I — A discussion of principles, J. Hydrol., 10(3), 282-290,1970.

535   Nguyen, H.H., Kim, H. and Choi, M.: Evaluation of the soil water content using cosmic-ray neutron probe in a heterogeneous monsoon climate-dominated region, Adv. Water Resour., 108, 125-138,2017.

Ni, L., Wang, D., Singh, V.P., Wu, J., Wang, Y. and Tao, Y. et al.: Streamflow and rainfall forecasting by two long short-term memory-based models, J. Hydrol., 583, 124296,2020.

Niroula, S., Halder, S. and Ghosh, S.: Perturbations in the initial soil moisture conditions: Impacts on hydrologic simulation
540   in a large river basin, J. Hydrol., 561, 509-522,2018.

Orth, R., Staudinger, M., Seneviratne, S.I., Seibert, J. and Zappa, M.: Does model performance improve with complexity? A case study with three hydrological models, J. Hydrol., 523, 147-159,2015.

Pablos, M., Turiel, A., Vall-Llossera, M., Camps, A. and Portabella, M., 2021. Correlated Triple Collocation to Estimate SMOS, SMAP and ERA5-Land Soil Moisture Errors. 2021 IEEE International Geoscience and Remote Sensing
545   Symposium IGARSS, pp. 6182-6185.

Palangi, H., Deng, L., Shen, Y., Gao, J., He, X. and Chen, J. et al.: Deep Sentence Embedding Using Long Short-Term Memory Networks: Analysis and Application to Information Retrieval, IEEE/ACM Transactions on Audio, Speech, and Language Processing, 24(4), 694-707,2016.

Paul, P.K., Kumari, B., Gaur, S., Mishra, A., Panigrahy, N. and Singh, R.: Application of a newly developed large‐scale
550   conceptual hydrological model in simulating streamflow for credibility testing in data scarce condition, Nat. Resour. Model., 33(4),2020.

Piazzi, G., Thirel, G., Perrin, C. and Delaigue, O.: Sequential Data Assimilation for Streamflow Forecasting: Assessing the Sensitivity to Uncertainties and Updated Variables of a Conceptual Hydrological Model at Basin Scale, Water Resour. Res., 57(4),2021.

555   Pourkarimi, L., Yaghoobi, M.A. and Mashinchi, M.: Efficient curve fitting: An application of multiobjective programming, Appl. Math. Model., 35(1), 346-365,2011.

Pradhan, N.R.: Estimating growing-season root zone soil moisture from vegetation index-based evapotranspiration fraction and soil properties in the Northwest Mountain region, USA, Hydrological Sciences Journal, 64(7), 771-788,2019.

Qi, D., Hu, T., Song, X. and Zhang, M.: Effect of nitrogen supply method on root growth and grain yield of maize under
560   alternate partial root-zone irrigation, Sci. Rep.-UK, 9(1),2019.

Refsgaard, J.C.: Parameterisation, calibration and validation of distributed hydrological models, J. Hydrol., 198(1-4), 69-97,1997.

Roulin, E. and Vannitsem, S.: Post-processing of medium-range probabilistic hydrological forecasting: impact of forcing,

initial conditions and model errors, Hydrol. Process., 29(6), 1434-1449,2015.

565 Senarath, S.U.S., Ogden, F.L., Downer, C.W. and Sharif, H.O.: On the calibration and verification of two-dimensional, distributed, Hortonian, continuous watershed models, Water Resour. Res., 36(6), 1495-1510,2000.

Seneviratne, S.I., Corti, T., Davin, E.L., Hirschi, M., Jaeger, E.B. and Lehner, I. et al.: Investigating soil moisture–climate interactions in a changing climate: A review, Earth-Sci. Rev., 99(3-4), 125-161,2010.

Setti, S., Maheswaran, R., Sridhar, V., Barik, K.K., Merz, B. and Agarwal, A.: Inter-Comparison of Gauge-Based Gridded

570 Data, Reanalysis and Satellite Precipitation Product with an Emphasis on Hydrological Modeling, Atmosphere-Basel, 11(11), 1152,2020.

Sherstinsky, A.: Fundamentals of Recurrent Neural Network (RNN) and Long Short-Term Memory (LSTM) network, Physica D: Nonlinear Phenomena, 404, 132306,2020.

Shrestha, S. and Kazama, F.: An export coefficient modeling approach to estimate organic matter and nutrient loadings from

575 point and non point sources into the Fuji river, Japan, Proceedings of the Symposium on Global Environment, 14, 21-26,2006.

Takeuchi, K., Ao, T. and Ishidaira, H.: Introduction of block-wise use of TOPMODEL and Muskingum-Cunge method for the hydroenvironmental simulation of a large ungauged basin, Hydrological Sciences Journal, 44(4), 633-646,1999.

Takeuchi, K., Hapuarachchi, P., Zhou, M., Ishidaira, H. and Magome, J.: A BTOP model to extend TOPMODEL for

580 distributed hydrological simulation of large basins, Hydrol. Process., 22(17), 3236-3251,2008.

Taylor, K.E.: Summarizing multiple aspects of model performance in a single diagram, Journal of Geophysical Research Atmospheres, 106(D7), 7183-7192,2001.

Ueng, W., Lai, J. and Tsai, Y.: Unconstrained and constrained curve fitting for reverse engineering, The International Journal of Advanced Manufacturing Technology, 33(11-12), 1189-1203,2007.

585 Vermote, E., Justice, C., Csiszar, I., Eidenshink, J., Myneni, R.B. and Baret, F. et al., NOAA Climate Data Record (CDR) of Normalized Difference Vegetation Index (NDVI), Version 4. NOAA National Centers for Environmental Information., https://doi.org/10.7289/V5PZ56R6.(accessed on Jun. 10 2021)

Wang, G., Hapuarachchi, H.A.P., Takeuchi, K. and Ishidaira, H.: Grid-based distribution model for simulating runoff and soil erosion from a large-scale river basin, Hydrol. Process., 24(5), 641-653,2010.

590 Wu, Z., Feng, H., He, H., Zhou, J. and Zhang, Y.: Evaluation of Soil Moisture Climatology and Anomaly Components Derived From ERA5-Land and GLDAS-2.1 in China, Water Resour. Manag., 35(2), 629-643,2021.

Yamazaki, D., Ikeshima, D., Tawatari, R., Yamaguchi, T., O'Loughlin, F. and Neal, J.C. et al.: A high-accuracy map of global terrain elevations, Geophys. Res. Lett., 44(11), 5844-5853,2017.

Yang, J., Qu, J., Mi, Q. and Li, Q.: A CNN-LSTM Model for Tailings Dam Risk Prediction, IEEE Access, 8, 206491-

595 206502,2020.

Yin, H., Zhang, X., Wang, F., Zhang, Y., Xia, R. and Jin, J.: Rainfall-runoff modeling using LSTM-based multi-state-vector sequence-to-sequence model, J. Hydrol., 598, 126378,2021.

Yu, D., Yang, J., Shi, L., Zhang, Q., Huang, K. and Fang, Y. et al.: On the uncertainty of initial condition and initialization approaches in variably saturated flow modeling, Hydrol. Earth Syst. Sci., 23(7), 2897-2914,2019.

600   Yu, Y., Si, X., Hu, C. and Zhang, J.: A Review of Recurrent Neural Networks: LSTM Cells and Network Architectures, Neural Comput., 31(7), 1235-1270,2019.

Zhang, H., Ao, T., Gusyev, M., Ishidaira, H., Magome, J. and Takeuchi, K.: Distributed source pollutant transport module based on BTOPMC: a case study of the Laixi River basin in the Sichuan province of southwest China, Proceedings of the International Association of Hydrological Sciences, 379, 323-333,2018.

605   Zhang, R., Li, L., Zhang, Y., Huang, F., Li, J. and Liu, W. et al.: Assessment of Agricultural Drought Using Soil Water Deficit Index Based on ERA5-Land Soil Moisture Data in Four Southern Provinces of China, Agriculture, 11(5), 411,2021.

Zhanlav, T. and Mijiddorj, R.: A comparative analysis of local cubic splines, Computational and Applied Mathematics, 37(5), 5576-5586,2018.

610   Zhou, L., Rasmy, M., Takeuchi, K., Koike, T., Selvarajah, H. and Ao, T.: Adequacy of Near Real-Time Satellite Precipitation Products in Driving Flood Discharge Simulation in the Fuji River Basin, Japan, Applied Sciences, 11(3), 1087,2021.

Zhou, M.C., Ishidaira, H., Hapuarachchi, H.P., Magome, J., Kiem, A.S. and Takeuchi, K.: Estimating potential evapotranspiration using Shuttleworth–Wallace model and NOAA-AVHRR NDVI data to feed a distributed
615   hydrological model over the Mekong River basin, J. Hydrol., 327(1-2), 151-173,2006.

Zhu, Y., Liu, L., Qin, F., Zhou, L., Zhang, X. and Chen, T. et al.: Application of the Regression-Augmented Regionalization Approach for BTOP Model in Ungauged Basins, Water-Sui., 13(16), 2294,2021.

620   **Tables**

Table 1 The variables of initial condition of BTOP model. The contents in bold are related soil moisture variables.

Filename	Units	File Descriptions	Default value
*.qi	m³/s	Initial/Input discharge to a grid at one time step	Based on observed
*.qo	m³/s	Initial/Output discharge from a grid at one time step	discharge and river route
*.sdbar	**m**	**Block average saturation deficit, calculated based on *SD(i)***	
*.srz	**m**	**Root zone storage for the selected time step**	
*.sto	m	River channel storage for the Manning's equation routing	
*.suz	**m**	**Unsaturated zone storage for the selected time step**	0
*.svz	m	Vegetation zone storage for the selected time step	
*.swz	m	Snow water equivalent for the snow module	

Table 2 The features of four hydrological simulation cases.

Case ID	Source of the SM initial condition	Warm-up	Calibration	Validation	Usage
Case 1	Default generated by model	2002			"Optimal" case
Case 2	Default generated by model	Null	2003-2007	2008-2011	Control case: without warm-up
Case 3	ERA5-Land with optimal curve fitting function	Null			Verifying ERA5-Land could be
Case 4	ERA5-Land with LSTM method	Null			used with proper process

Table 3 The six curve fitting functions used in this study.

Curve types	Degree (d)	Functions	Knot number (k)	Restrictions
Polynomial	1, 2, 3, 4	$C(u) = a_0 u^d + a_1 u^{d-1} + a_2 u^{d-2} + \cdots + a_d u^0$	/	/
Natural Logarithmic	/	$C(u) = a_0 + a_1 \ln a_2 u$	/	/
Natural cubic spline	3	$C(u) = \sum_{i=0}^{k} a_i S_{3,i}(u)$	3	$S_{3,i}(t_j) = S_{3,i+1}(t_j)\ S'_{3,i}(t_j) = S'_{3,i+1}(t_j)$ $S''_{3,i}(t_j) = S''_{3,i+1}(t_j)$ $S_3''(a) = S_3''(b) = S_3'''(a) = S_3'''(b) = 0$

Note: a_i is the constant value; u is the independent variable. For the spline function, consider the interval $[a, b]$ divided by k nodes into $k+1$ pieces, $S_{3,i}(u)$ is the cubic polynomial of the i-th piece and $t_j\ (1 \le j \le k)$ is the j-th knot.

625

Table 4 The performance score of curve fitting functions for developing the relationship of SM variables in FRB and SRB. The bold numbers are the highest scores in different basins.

SM variables	Basins	Polynomial $(d = 1)$	Polynomial $(d = 2)$	Polynomial $(d = 3)$	Polynomial $(d = 4)$	Logarithmic	Natural cubic spline
S_{rz}	FRB	0.188	0.641	0.404	0.501	0.333	**0.739**
	SRB	0.443	0.663	0.353	0.512	0.437	**0.719**
SD	FRB	0.355	**0.734**	0.641	0.657	0.405	0.722
	SRB	0.371	**0.760**	0.678	0.696	0.398	0.346
S_{uz}	FRB	**0.741**	0.639	0.510	0.363	0.499	0.610
	SRB	0.654	**0.803**	0.710	0.260	0.698	0.715

Figures
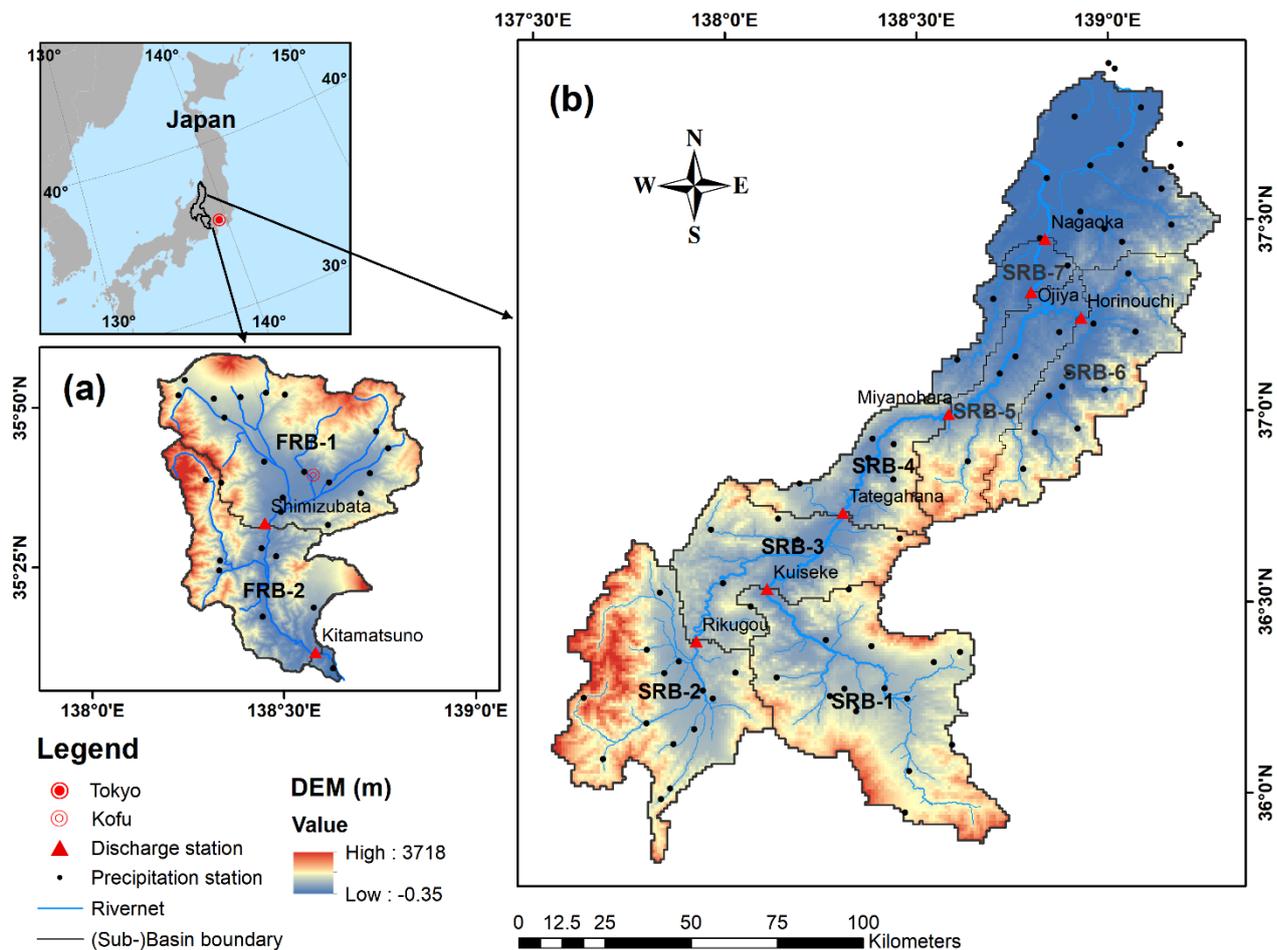
Figure 1 The location, DEM, ground observation, and sub-basin of study areas. (a) The Fuji River Basin (FRB); (b) The Shinano River Basin (SRB). Sub-basins are denoted as FRB-1, SRB-1, etc.

630

26
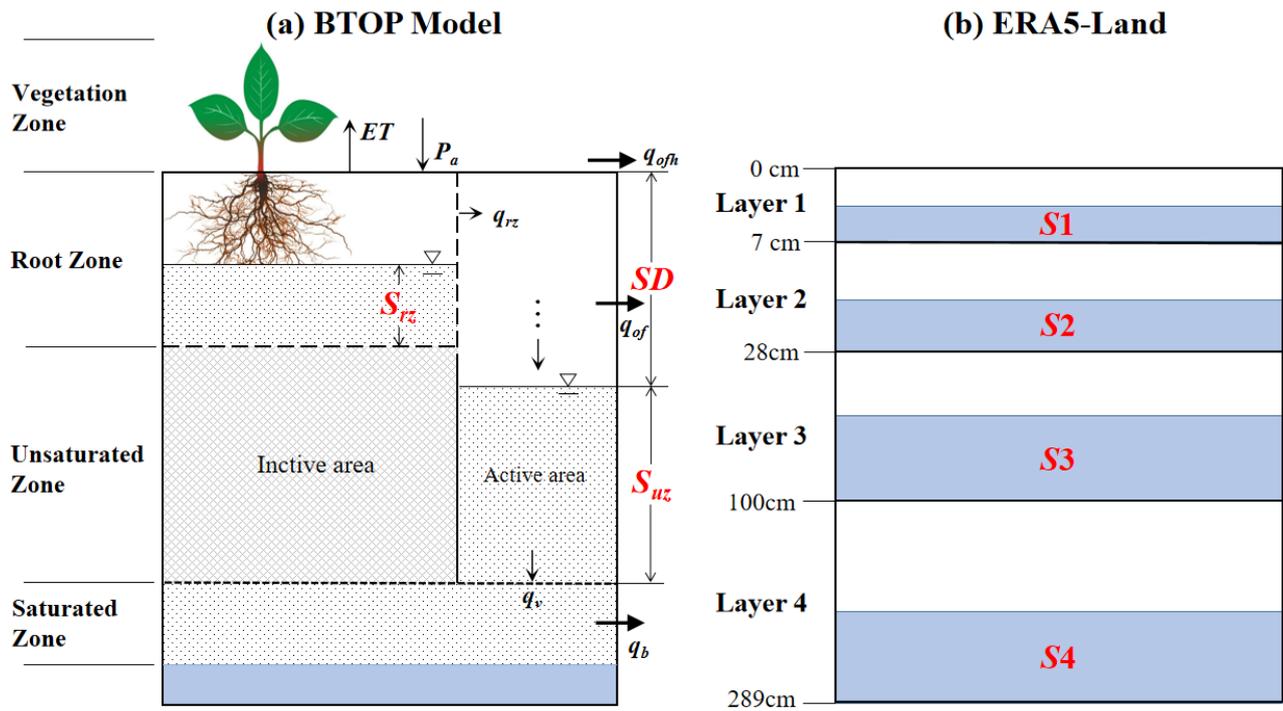
Figure 2 The structure of soil moisture variables in BTOP and ERA5-Land. (a) The theoretical concept of the BTOP model (modified from Takeuchi et al. (2008), Figure 3); (b) The soil moisture structure (four layers) of EAR5-Land.
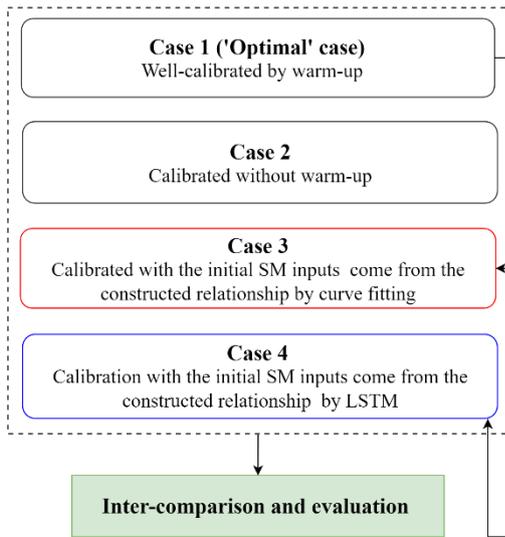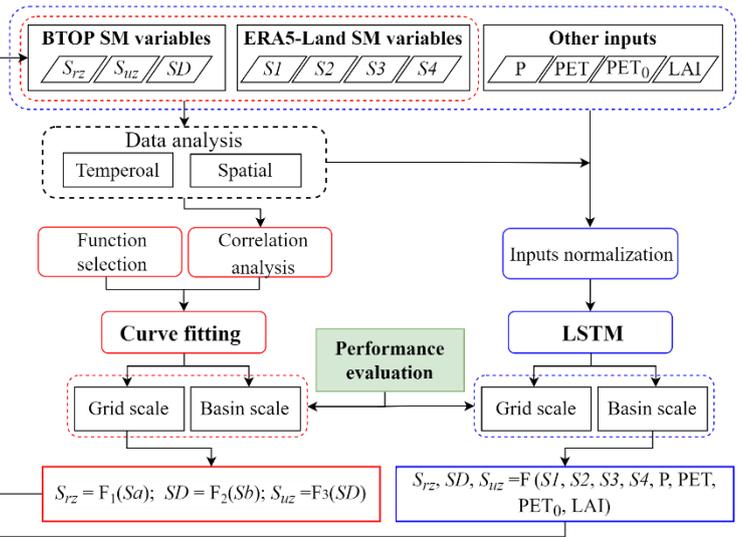
Figure 3 Framework of this study.

635
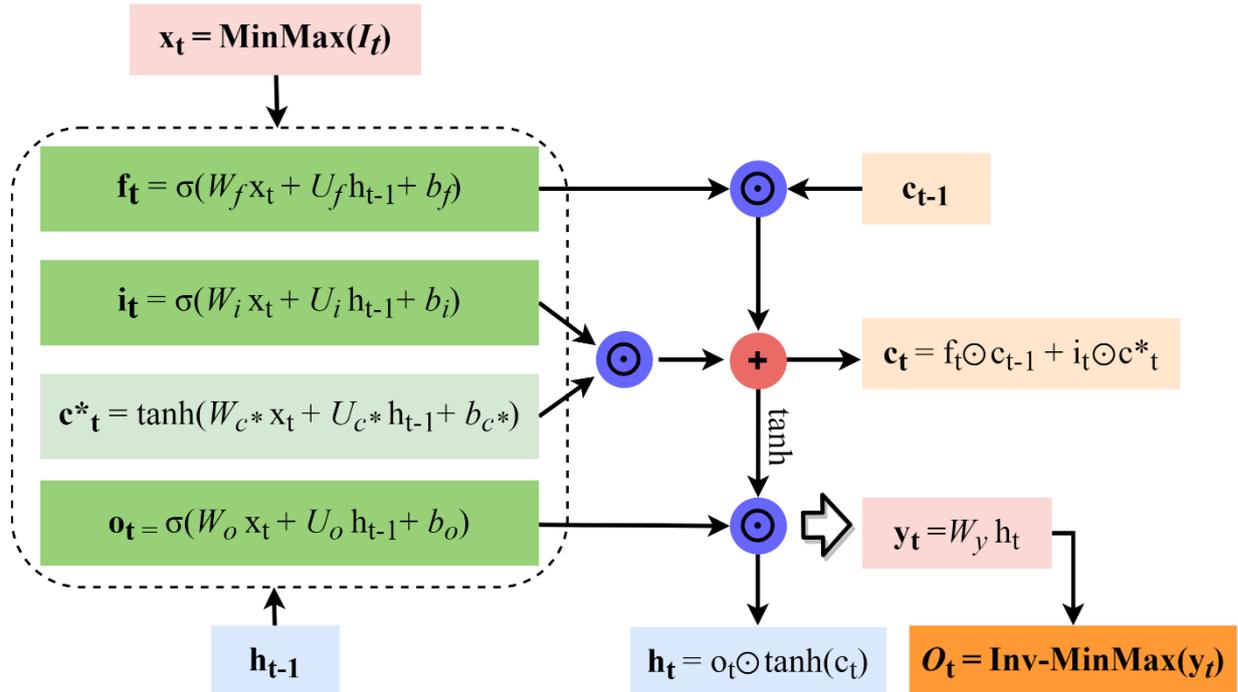
Figure 4 Schematic diagram of long-short term memory (LSTM). W, U and b are the input weights, cyclic weights and bias, respectively. c_t, $c*_t$ and h_t are cell state, candidate cell state and hidden state. i_t, f_t and o_t are input gate, forget gate and output gate. x_t and y_t are normalized input I_t and output O_t. $\oplus$ and $\odot$ are for matrix addition and multiplication respectively.
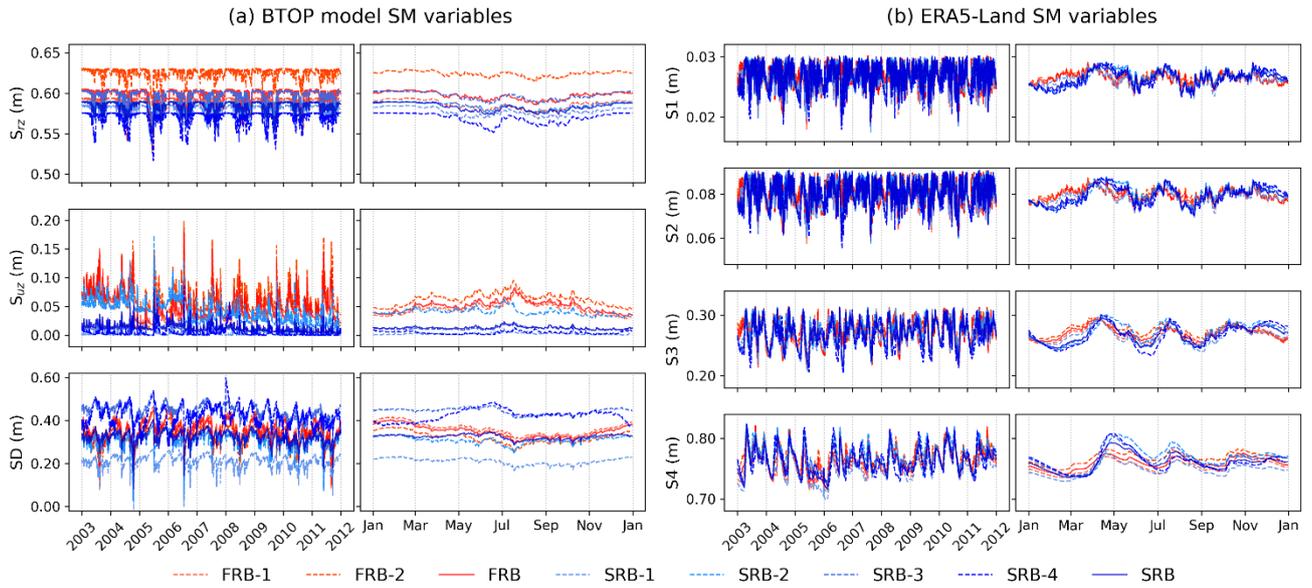
Figure 5 Temporal performance of BTOP model and EAR5-Land SM variables at daily and annual average daily scale in each (sub-) basins. (a) BTOP model SM variables: S_{rz}, S_{uz}, and SD. (b) ERA5-Land SM variables: $S1$, $S2$, $S3$, and $S4$.
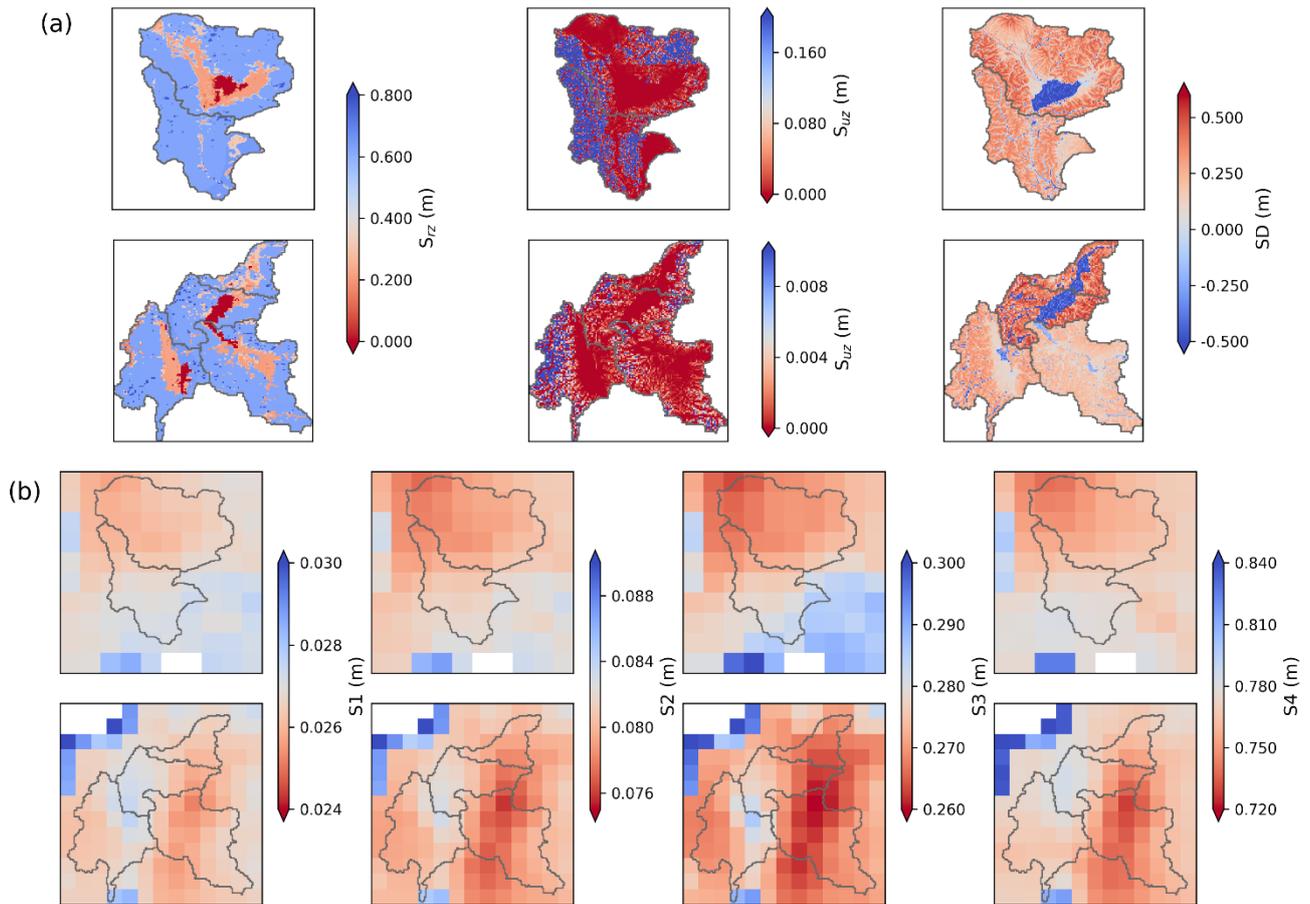
Figure 6 Spatial performance of the annual average SM variables in the study areas. (a) BTOP model SM variables: *Suz* and *Srz*, *SD*. The resolutions for FRB and SRB are 500 m and 1000 m, respectively. (b) ERA5-Land SM variables: *S1*, *S2*, *S3*, and *S4*. The resolution is 0.1º, approximately 9 km.

640
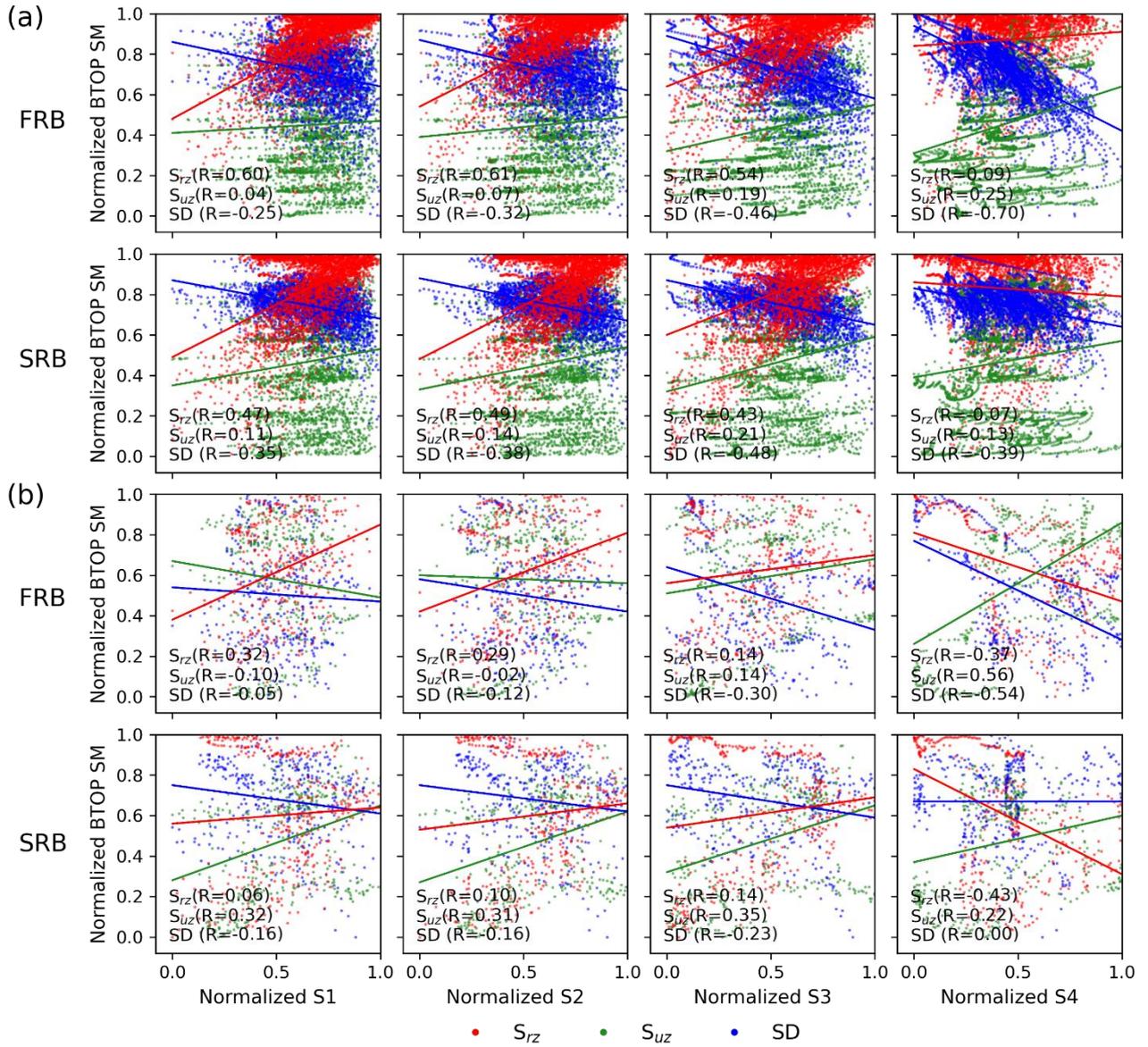
Figure 7 Scatterplots and correlation results of the various normalized SM variable combinations in EXP 1 (i.e., the successive combination of *Srz*, *Suz*, and *SD* with *S1*, *S2*, *S3*, and *S4*) daily and annual average daily scale for FRB and SRB. (a) Daily scale; (b) Annual average daily scale. The values in the figure are processed using Min-max normalization technical.
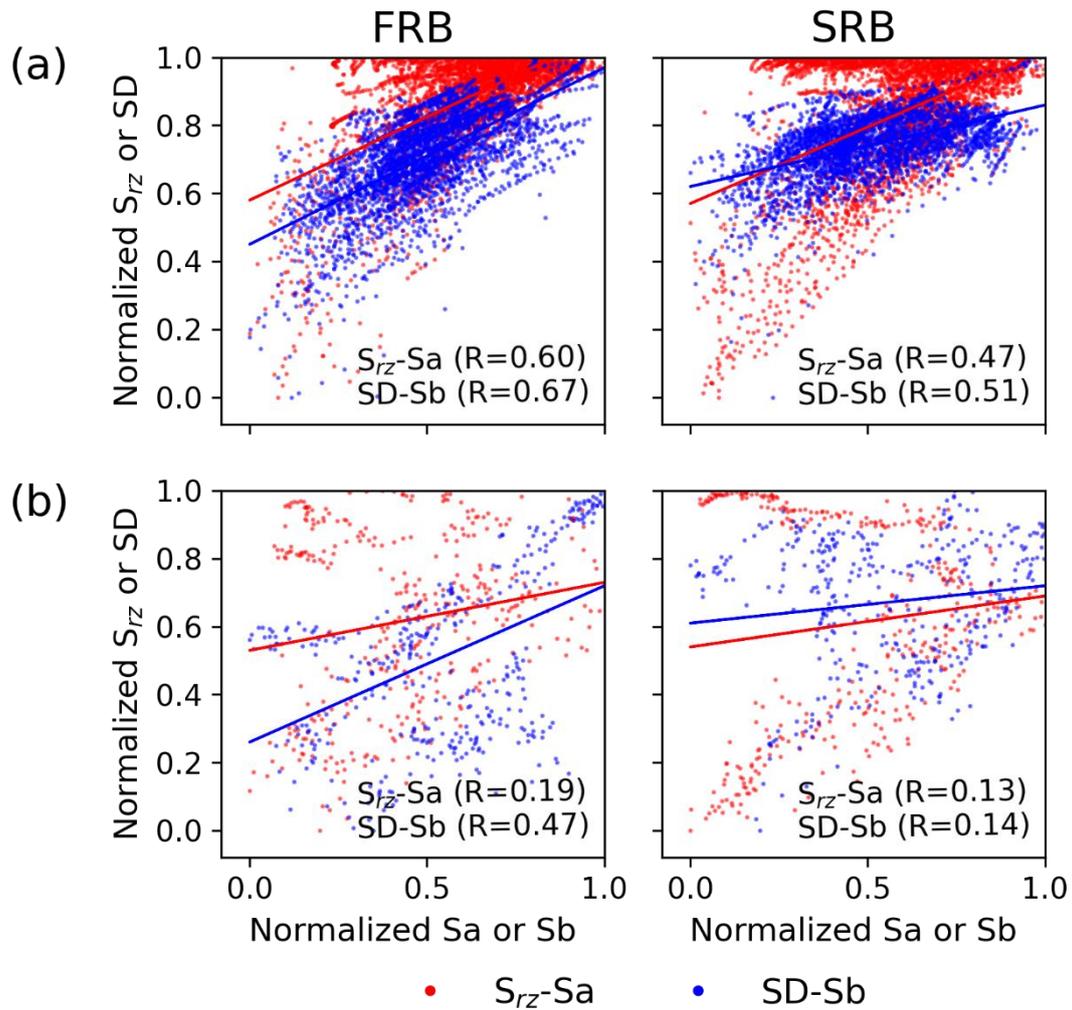
Figure 8 Scatterplots and correlation results of S_{rz}-Sa and SD-Sb in EXP 2 in FRB and SRB. (a) and (b) represent the correlations at daily scale and annual average daily scale, respectively. Sa equals the sum of $S1$, $S2$, and $S3$, while Sb equals Depth (289 cm) minus Sa. The values in the figure are processed using Min-max normalization technical.

645
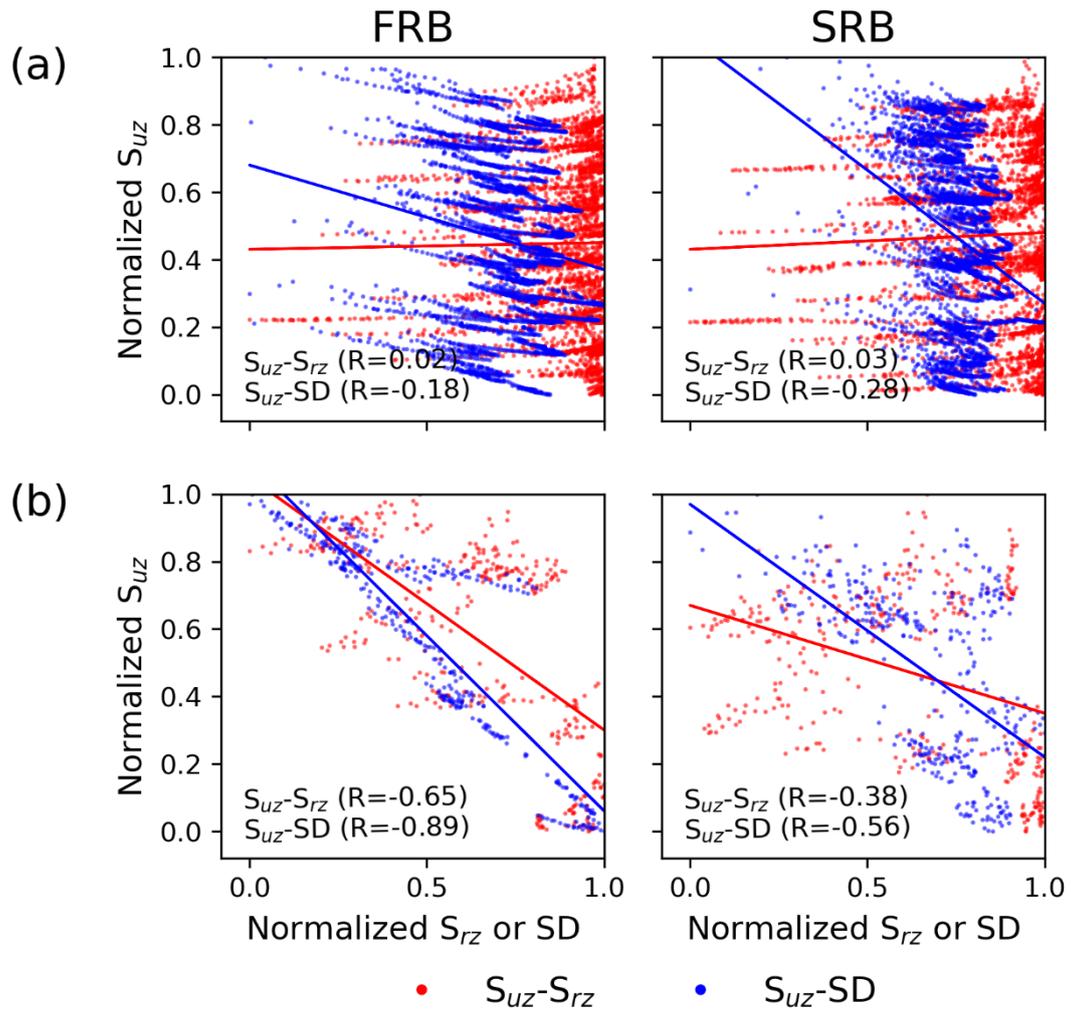
Figure 9 Scatterplots and correlation results of S_{uz}-S_{rz} and S_{uz}-SD in EXP 3 in FRB and SRB. (a) and (b) represent daily scale and annual average daily scale, respectively. The values in the figure are processed using Min-max normalization technical.
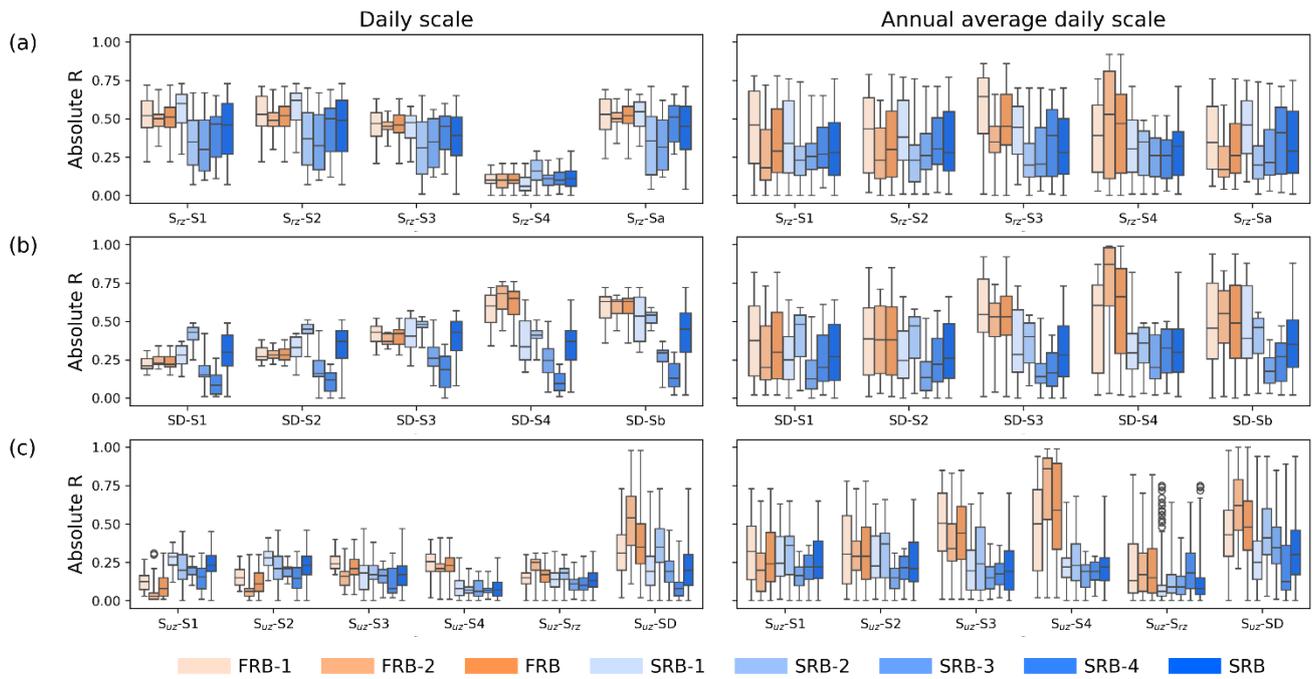
Figure 10 Boxplots of absolute correlation coefficient values (R) between BTOP SM variables (S_{rz}, SD, and S_{uz}) and corresponding SM variables in grid cells at daily and annual average daily scale. (a) S_{rz}; (b) SD; (c) S_{uz}.
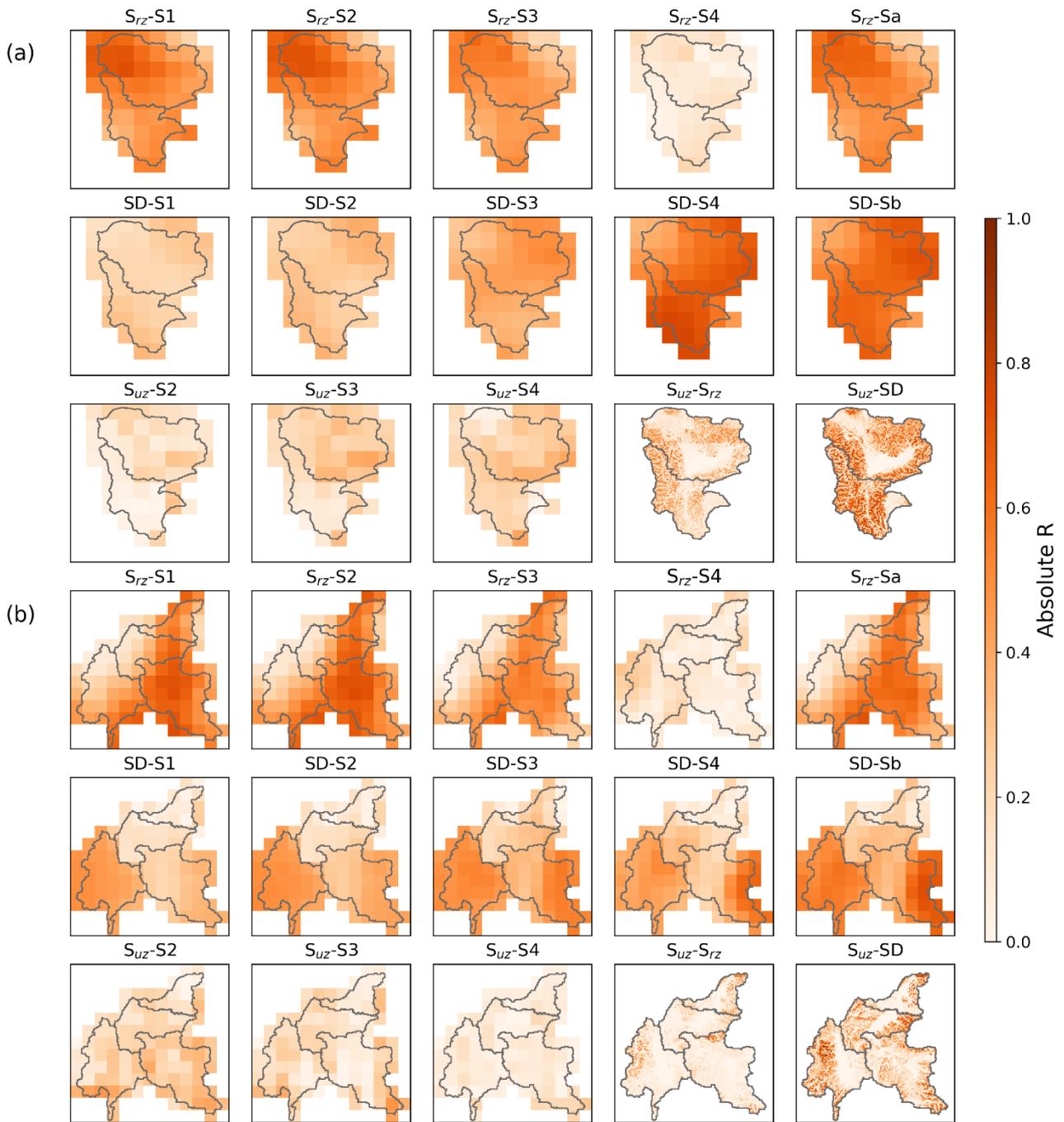
Figure 11 Spatial distribution of the absolute correlation coefficient (R) between S_{rz}, SD, and S_{uz} and corresponding SM variables in the study areas. (a) FRB; (b) SRB. R values of S_{uz}-S_{rz} and S_{uz}-SD are obtained from the annual average daily series at BTOP model resolution, while the rest are daily series at 0.1°. S_{uz} has five relationships, and its correlation with $S1$ is the worst, which is not shown here for layout purposes.

650
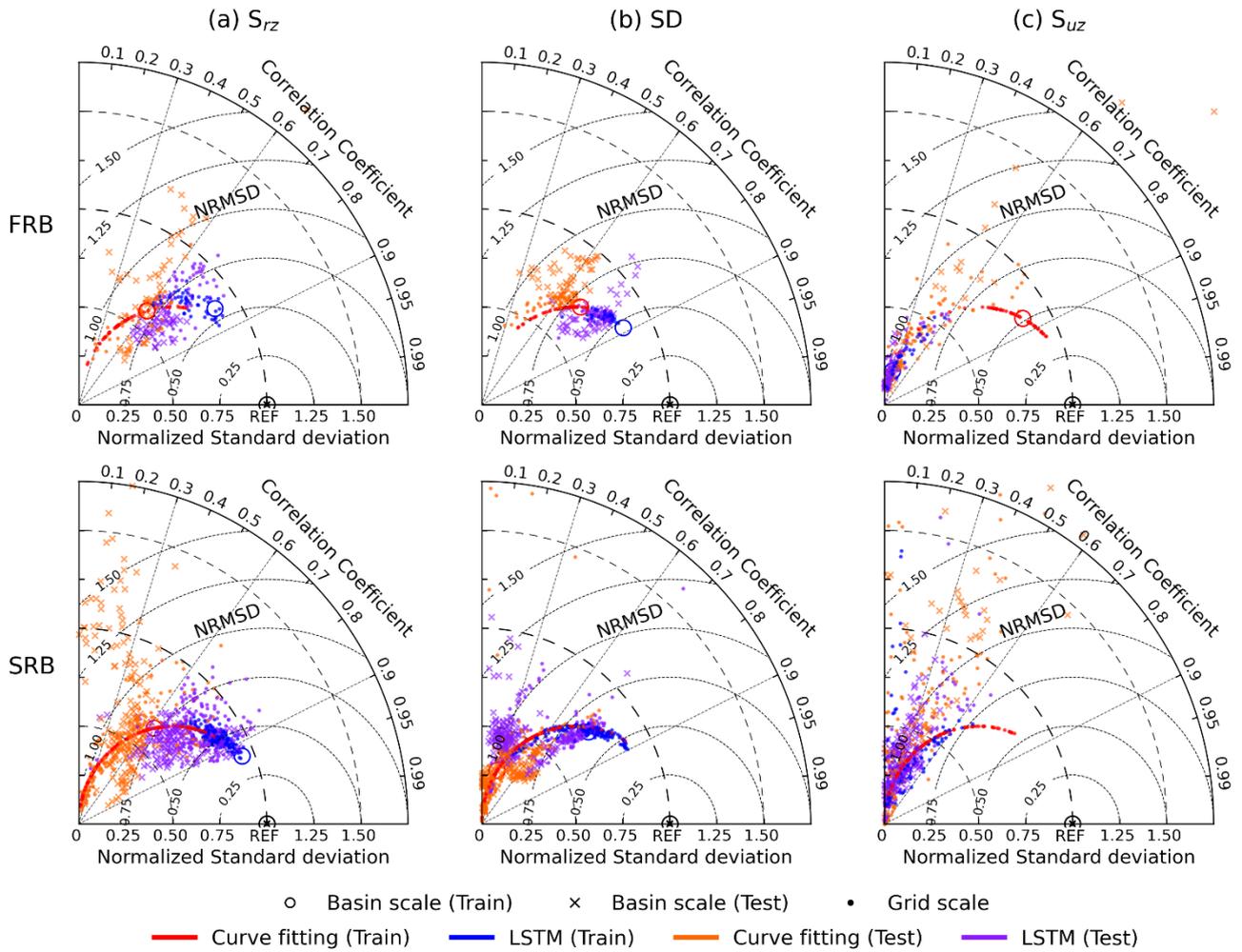
Figure 12 Talyor diagram of the corresponding optimal curve fitting functions and LSTM in relationship development at basin- and grid-scales during the training and test period for BTOP SM variables. (a) S_{rz}; (b) SD; (c) S_{uz}. The REF comes from the outputs of Caes 1 that simulated with warm-up. The training periods are shown in red and blue for curve fitting and LSTM, respectively, while orange and purple represent the test periods. The hollow circle denotes the training at basin scale, and its test results are shown by cross markers at grid-scale. Small dots represent the grid-scale results in both training and test periods.
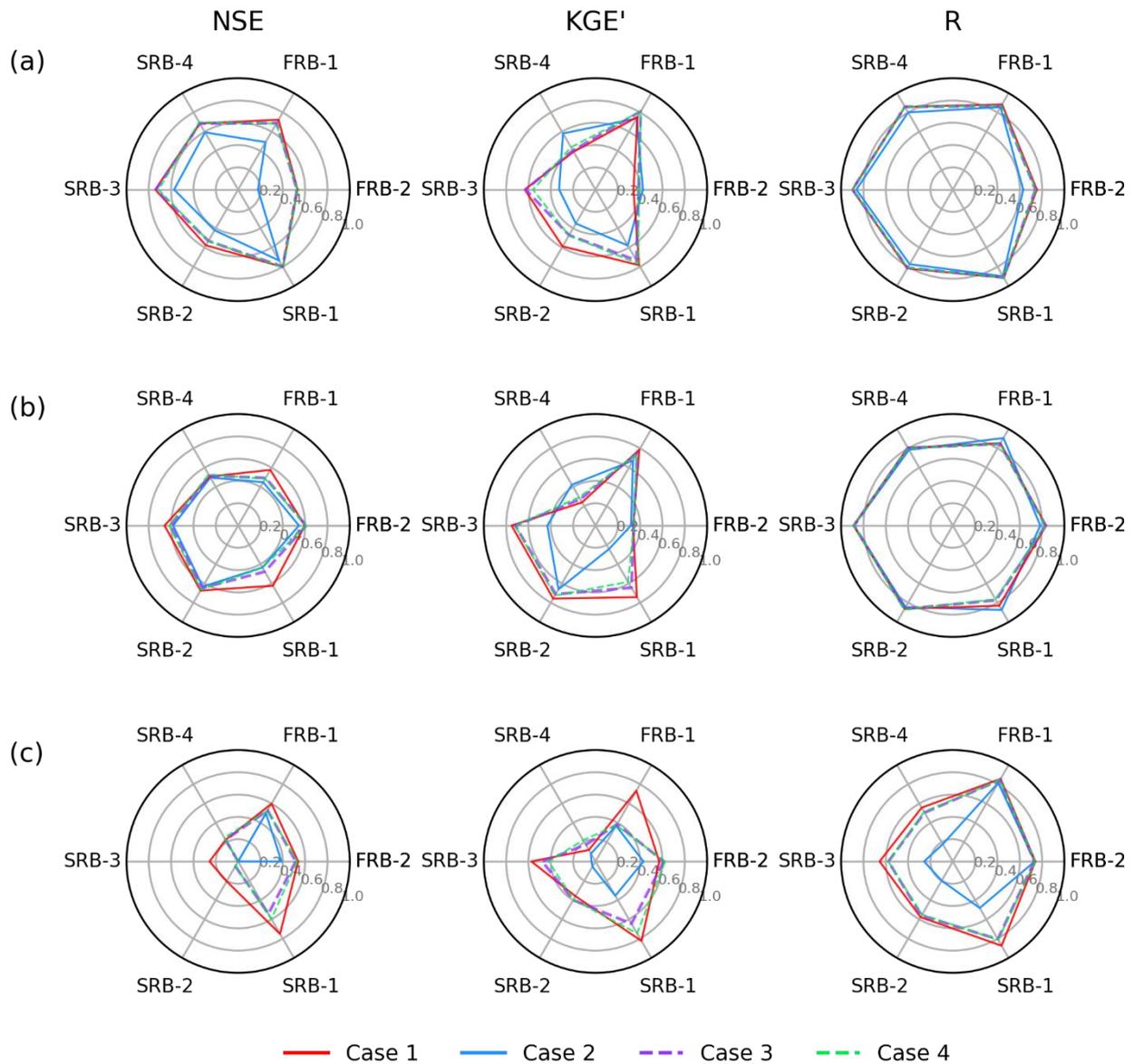
Figure 13 Performance evaluation of four configured hydrological simulations cases with NSE, KGE' and R. (a) Calibration period; (b) Validation period; (c) Year 2003. The negative values are modified to zero to show the apparent shape of the results. Case 1 is the optimal case with a warm-up. Case 2 is the control case without warm-up. Case 3 and 4 are the cases with initial conditions that come from optimal curve fitting function and LSTM, respectively.